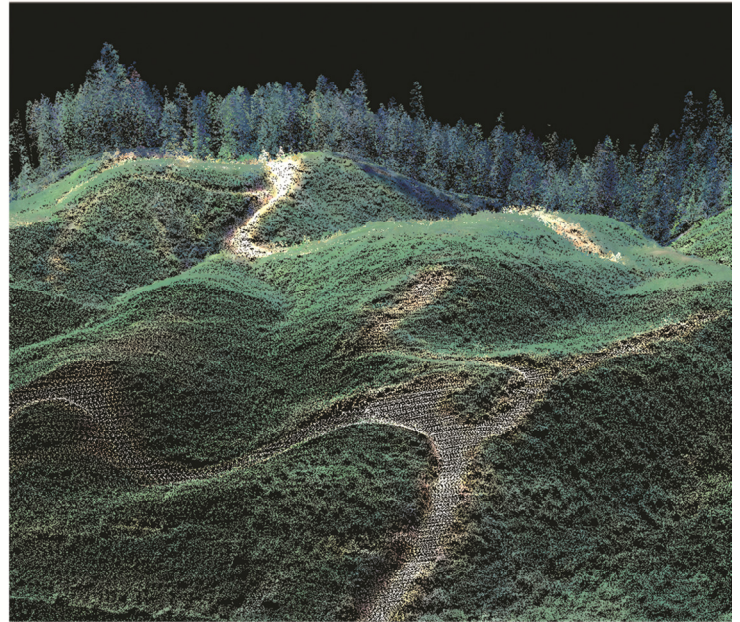


LiDAR REMOTE SENSING

CLEARWATER • IDAHO

(DELIVERY 2 - 11/07/2011)



USDA NEZ PERCE NATIONAL FOREST

BILL CONROY - 104 Airport Road - Grangeville, Idaho 83530

 WATERSHED SCIENCES • 517 SW 2nd Street, Suite 400 - Corvallis, OR 97333

LIDAR REMOTE SENSING DATA COLLECTION: CLEARWATER, ID (DELIVERY 2)

TABLE OF CONTENTS

1. Overview	1
2. Acquisition	2
2.1 Airborne Survey - Instrumentation and Methods	2
2.2 Ground Survey - Instrumentation and Methods	3
2.2.1 Instrumentation	3
2.2.2 Monumentation	3
2.2.3 Methodology	4
3. LiDAR Data Processing	13
3.1 Applications and Work Flow Overview	13
3.2 Aircraft Kinematic GPS and IMU Data	13
3.3 Laser Point Processing	14
4. LiDAR Accuracy Assessment	15
4.1 Laser Noise and Relative Accuracy	15
4.2 Absolute Accuracy	16
5. Study Area Results	16
5.1 Data Summary: Laundry China Osier	17
5.1.1 Data Density/Resolution	17
5.1.2 Relative Accuracy Calibration Results	21
5.1.3 Absolute Accuracy	22
5.1.4 Accuracy per Land Cover	23
5.2 Data Summary: Walde Pete King	24
5.2.1 Data Density/Resolution	24
5.2.2 Relative Accuracy Calibration Results	28
5.2.3 Absolute Accuracy	29
5.2.4 Accuracy per Land Cover	30
5.3 Data Summary: Upper Elk	30
5.3.1 Data Density/Resolution	30
5.3.2 Relative Accuracy Calibration Results	34
5.3.3 Absolute Accuracy	35
5.3.4 Accuracy per Land Cover	36
5.4 Data Summary: Potlatch	36
5.4.1 Data Density/Resolution	36
5.4.2 Relative Accuracy Calibration Results	39
5.4.3 Absolute Accuracy	40
5.4.4 Accuracy per Land Cover	41
5.5 Data Summary: Musselshell	41
5.5.1 Data Density/Resolution	41
5.5.2 Relative Accuracy Calibration Results	44
5.5.3 Absolute Accuracy	45

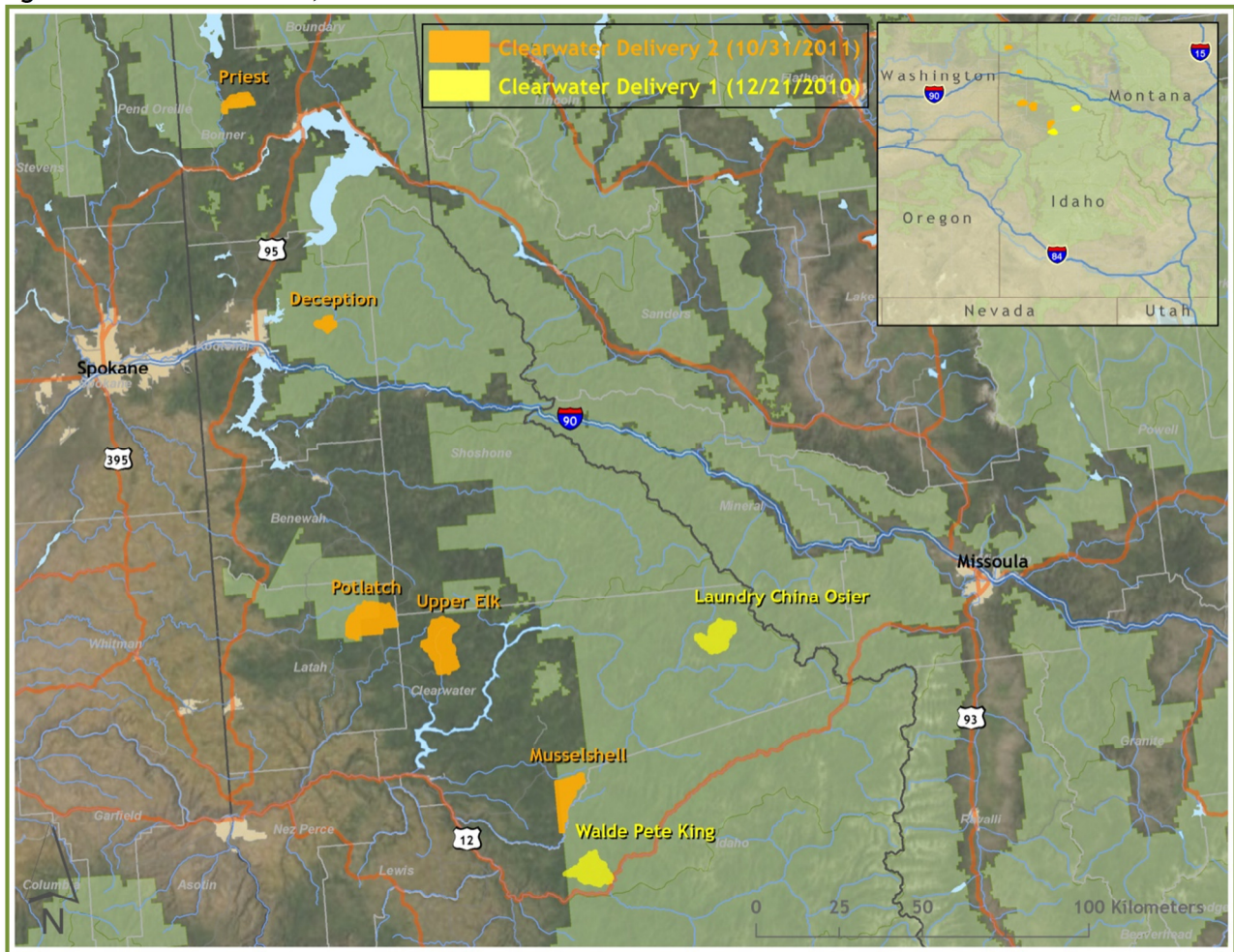
5.5.4 Accuracy per Land Cover	46
5.6 Data Summary: Priest.....	46
5.6.1 Data Density/Resolution	46
5.6.2 Relative Accuracy Calibration Results	49
5.6.3 Absolute Accuracy.....	50
5.6.4 Accuracy per Land Cover	51
5.7 Data Summary: Deception	51
5.7.1 Data Density/Resolution	51
5.7.2 Relative Accuracy Calibration Results	54
5.7.3 Absolute Accuracy.....	55
5.7.4 Accuracy per Land Cover	56
6. Projection/Datum and Units	57
7. Deliverables	57
8. Selected Images	58
9. Glossary	63
10. Citations	64
Appendix A.....	65



1. Overview

Watershed Sciences, Inc. (WS) collected Light Detection and Ranging (LiDAR) data for Delivery 2 of the Clearwater project from July 27th through the 30th, 2011. This report documents the data acquisition, processing methods, accuracy assessment, and deliverables for the first delivery (2010) AOs (*Laundry China Osier* -17,614 Acres; *Walde Pete King* - 15,452 Acres) as well as the remaining Delivery 2 (2011) AOs (*Upper Elk* -28,260 acres, *Potlatch* -27,174 acres, *Musselshell* -15,975 acres, *Priest* -6,986 acres, and *Deception* -3,953 acres). The requested areas were expanded to include a 100m buffer to ensure complete coverage and adequate point densities around survey area boundaries resulting in a total of 35,081 and 82,348 acres for deliveries 1 and 2 respectively.

Figure 1. Clearwater AOs, Deliveries 1 & 2



2. Acquisition

2.1 Airborne Survey - Instrumentation and Methods

The 2011 LiDAR survey utilized dual-mounted Leica ALS50 Phase II sensors in a Cessna Caravan 208B. The ALS50ii sensor operates with Automatic Gain Control (AGC) for intensity correction. The Leica systems were set to acquire 73500 laser pulses per second (i.e., 73.5K pulse rate) and flown at 1500 meters above ground level (AGL), capturing a scan angle of $\pm 15^\circ$ from nadir (partial settings for 7/27/2011 were 88 kHz pulse rate flown at 1200 meters (Potlatch AOI)). With these flight parameters, the laser swath width is ~800m and the laser pulse footprint is ~34cm. These settings were developed to yield points with an average native pulse density of ≥ 4 pulses per square meter over terrestrial surfaces. It is not uncommon for some types of surfaces (e.g. dense vegetation or water) to return fewer pulses than the laser originally emitted. These discrepancies between 'native' and 'delivered' density will vary depending on terrain, land cover, and the prevalence of water bodies.



The Cessna Caravan is a stable platform, ideal for flying slow and low for high density projects. A Leica ALS50ii sensor head installed in the Caravan is shown on the left.

All areas were surveyed with an opposing flight line side-lap of $\geq 50\%$ ($\geq 100\%$ overlap) to reduce laser shadowing and increase surface laser painting. The Leica laser systems allow up to four range measurements (returns) per pulse, and all discernable laser returns were processed for the output dataset.

To accurately solve for laser point position (geographic coordinates x, y, z), the positional coordinates of the airborne sensor and the attitude of the aircraft were recorded continuously throughout the LiDAR data collection mission. Aircraft position was measured twice per second (2 Hz) by an onboard differential GPS unit. Aircraft attitude was measured 200 times per second (200 Hz) as pitch, roll and yaw (heading) from an onboard inertial measurement unit (IMU). To allow for post-processing correction and calibration, aircraft/sensor position and attitude data are indexed by GPS time.

2.2 Ground Survey - Instrumentation and Methods

During the LiDAR survey, static (1 Hz recording frequency) ground surveys were conducted over set monuments. Monument coordinates are provided in **Table 1** and shown in **Figures 2-8** for the AOIs. After the airborne survey, the static GPS data were processed using triangulation with Continuously Operating Reference Stations (CORS) and checked using the Online Positioning User Service (OPUS¹) to quantify daily variance. Multiple sessions were processed over the same monument to confirm antenna height measurements and reported position accuracy.

Indexed by time, these GPS data were used to correct the continuous onboard measurements of aircraft position recorded throughout the mission. Control monuments were located within 13 nautical miles of the survey area.



2.2.1 Instrumentation

For this project, a Trimble GPS receiver model R7 with Zephyr Geodetic antenna with ground plane was deployed for all static control. A Trimble model R8 GNSS unit was used for collecting check points using real time kinematic (RTK) survey techniques. For RTK data, the collector began recording after remaining stationary for 5 seconds then calculating the pseudo range position from at least three epochs with the relative error under 1.5cm horizontal and 2cm vertical. All GPS measurements were made with dual frequency L1-L2 receivers with carrier-phase correction.

2.2.2 Monumentation

Watershed Sciences established seventeen monuments for both Delivery 1 and Delivery 2 of the Clearwater Remote Sensing LiDAR project. The Watershed Sciences' monumentation was done with 5/8" x 30" rebar topped with a metal cap stamped with "Watershed Sciences, Inc," the monument ID, and the year of establishment. Whiteshield Inc., Pasco, WA (ID Professional Land Surveyor, Michael LeJeune (PLS #5002) provided the professional oversight and control certification for the project. The survey control report is included on the delivery drive. The PLS certified nine of the seventeen control points used for this dataset, and the remaining eight were used for redundancy (see Table 1 and survey control report).

¹ Online Positioning User Service (OPUS) is run by the National Geodetic Survey to process corrected monument positions.

Table 1. Base Station control coordinates for all AOIs in Delivery 1 & 2 of the Clearwater 2011 remote sensing project.

Base Station ID	Datum: NAD83 (CORS96)		GRS80
	Latitude	Longitude	Ellipsoid Z (meters)
CHIN_01	46 50 49.73711 N	115 05 37.34969 W	1073.279
CHIN_02	46 48 24.37557 N	115 01 50.99768 W	1515.745
WALDE_01	46 14 39.18988 N	115 48 46.33587 W	957.820
WALDE_02	46 15 33.33651 N	115 46 13.81605 W	1039.891
WALDE_03	46 14 40.08771 N	115 49 16.18893 W	937.846
WALDE_05	46 14 09.96646 N	115 40 34.57108 W	1261.942
ELK_01	46 47 28.03207 N	116 10 26.76396 W	844.773
ELK_02	46 53 12.28987 N	116 09 24.84872 W	1046.675
BOVL_GPS	46 51 24.49623 N	116 24 07.29811 W	856.158
POT_01	46 54 25.13355 N	116 23 30.60214 W	867.634
MUSS_01	46 21 06.34281 N	115 45 32.11941 W	949.849
DECEP_01	47 43 12.94544 N	116 32 14.10221 W	1238.172
DECEP_02	47 43 45.60301 N	116 32 57.32176 W	1330.289
DECEP_03	47 43 16.30536 N	116 30 00.10162 W	1191.284
AC5222	48 17 39.13444 N	116 33 50.26816 W	631.190
PRIEST_02	48 21 43.04027 N	116 50 25.03881 W	670.917
PRIEST_03	48 20 01.11979 N	116 50 44.49634 W	671.304

2.2.3 Methodology



Each aircraft is assigned a ground crew member with two Trimble R7 receivers and an R8 receiver. The ground crew vehicles are equipped with standard field survey supplies and equipment including safety materials. All control monuments are observed for a minimum of two survey sessions lasting no fewer than 6 hours. At the beginning of every session the tripod and antenna are reset, resulting in two independent instrument heights and data files. Data is collected at a rate of 1Hz using a 10 degree mask on the antenna.

The ground crew uploads the GPS data to our Dropbox website on a daily basis to be returned to the office for QA/QC review and processing. OPUS processing triangulates the monument position using 3 CORS stations resulting in a fully adjusted position. After multiple days of data have been collected at each monument, accuracy and error ellipses

are calculated from the OPUS reports. This information leads to a rating of the monument based on FGDC-STD-007.2-1998² Part 2 table 2.1 at the 95% confidence level. When a statistical stable position is found CORPSCON³ 6.0.1 software is used to convert the UTM positions to geodetic positions. This geodetic position is used for processing the LiDAR data.

RTK and aircraft mounted GPS measurements are made during periods with PDOP⁴ less than or equal to 3.0 and with at least 6 satellites in view of both a stationary reference receiver and the roving receiver. Static GPS data collected in a continuous session average the high PDOP into the final solution in the method used by CORS stations. RTK positions are collected on bare earth locations such as paved, gravel or stable dirt roads, and other locations where the ground is clearly visible (and is likely to remain visible) from the sky during the data acquisition and RTK measurement period(s). RTK positions were also taken in several different habitat types in each AOI (grass, shrub, trees, and a few wetlands) and the results from these vegetation check point sessions are reported at the end of each AOI data summary.

In order to facilitate comparisons with LiDAR measurements, RTK measurements are not taken on highly reflective surfaces such as center line stripes or lane markings on roads. RTK points were taken no closer than one meter to any nearby terrain breaks such as road edges or drop offs.



² Federal Geographic Data Committee Draft Geospatial Positioning Accuracy Standards

³ U.S. Army Corps of Engineers , Engineer Research and Development Center Topographic Engineering Center software

⁴PDOP: Point Dilution of Precision is a measure of satellite geometry, the smaller the number the better the geometry between the point and the satellites.

LiDAR Data Acquisition and Processing: Clearwater, ID: Delivery 2

Prepared by Watershed Sciences, Inc.

Figure 2. RTK check points, land cover check points, and control monument locations used in the Laundry China Osier AOI.

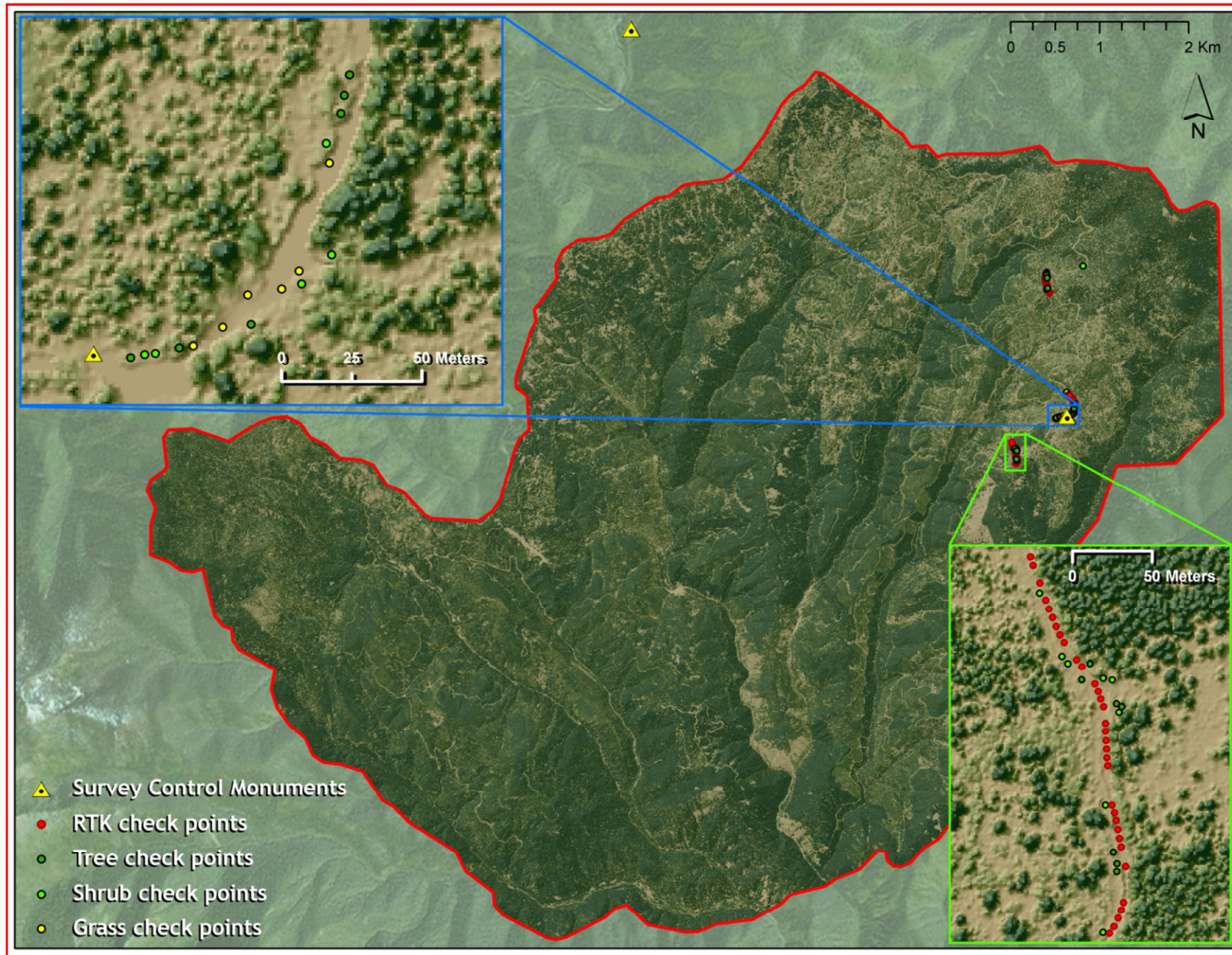


Figure 3. RTK check point, land cover check points, and control monument locations used in the Walde Pete King AOI.

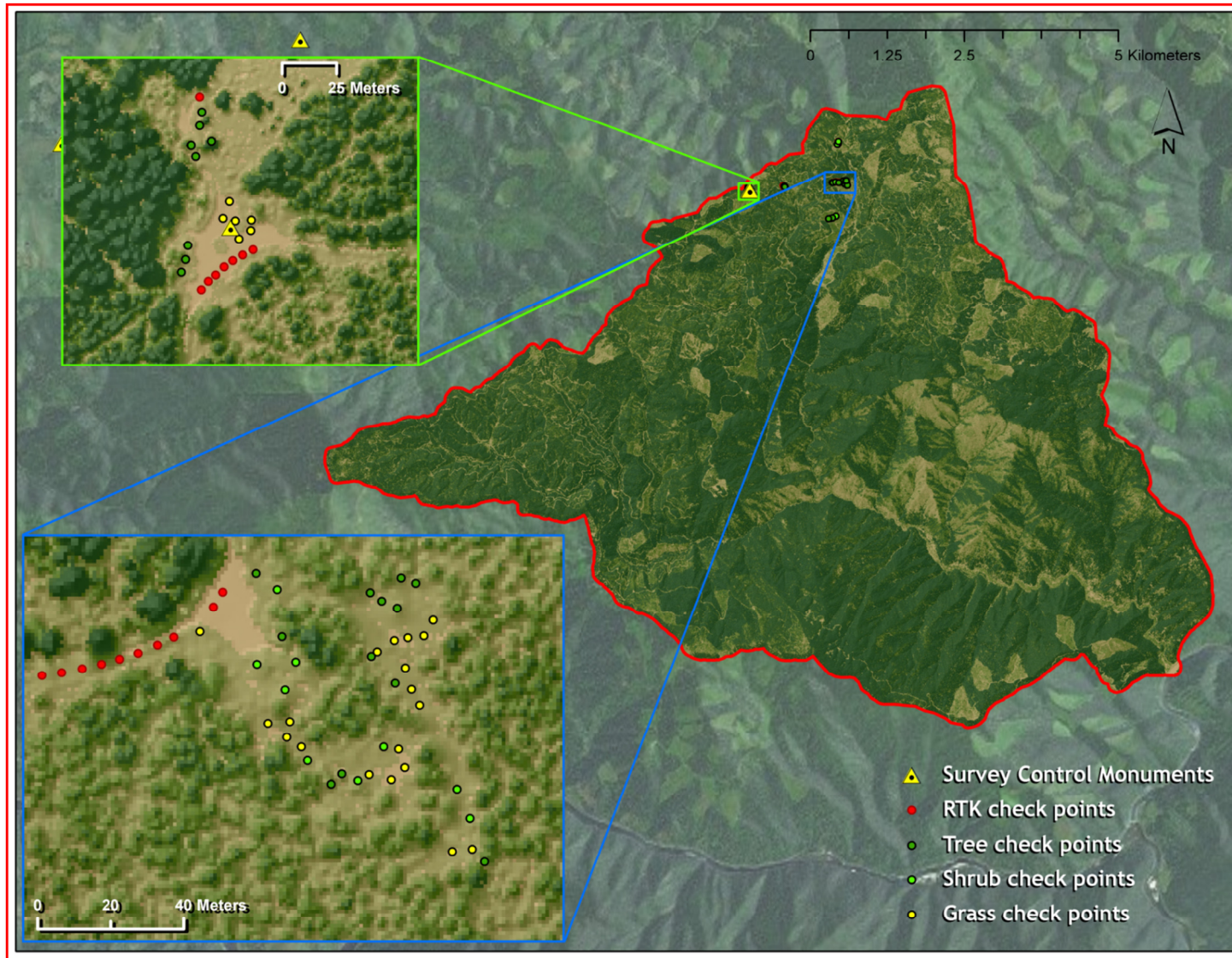


Figure 4. RTK check point, land cover check points, and control monument locations used in the Upper Elk AOI.

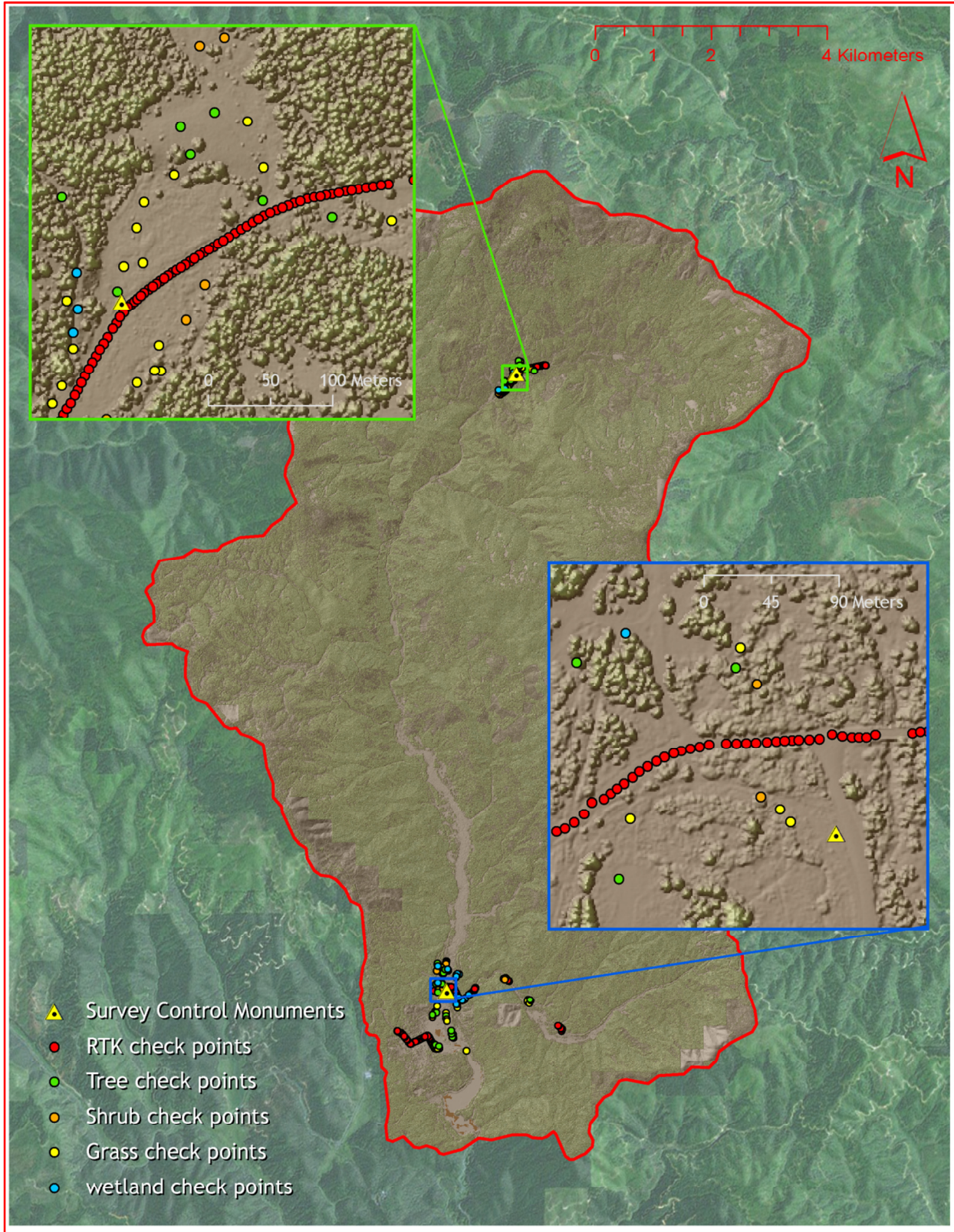


Figure 5. RTK check point, land cover check points, and control monument locations used in the Potlatch AOI.

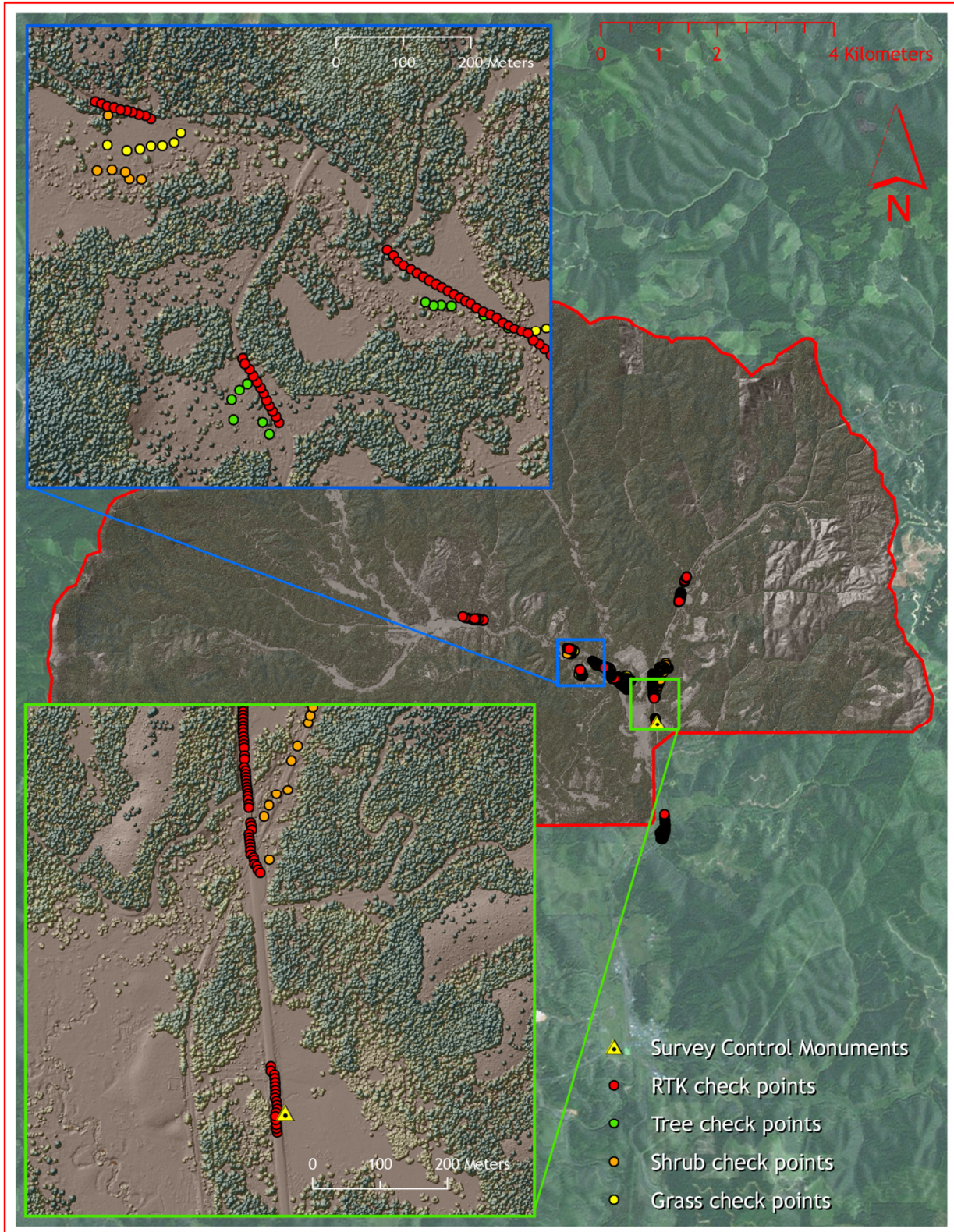


Figure 6. RTK check point, land cover check points, and control monument locations used in the Musselshell AOI.

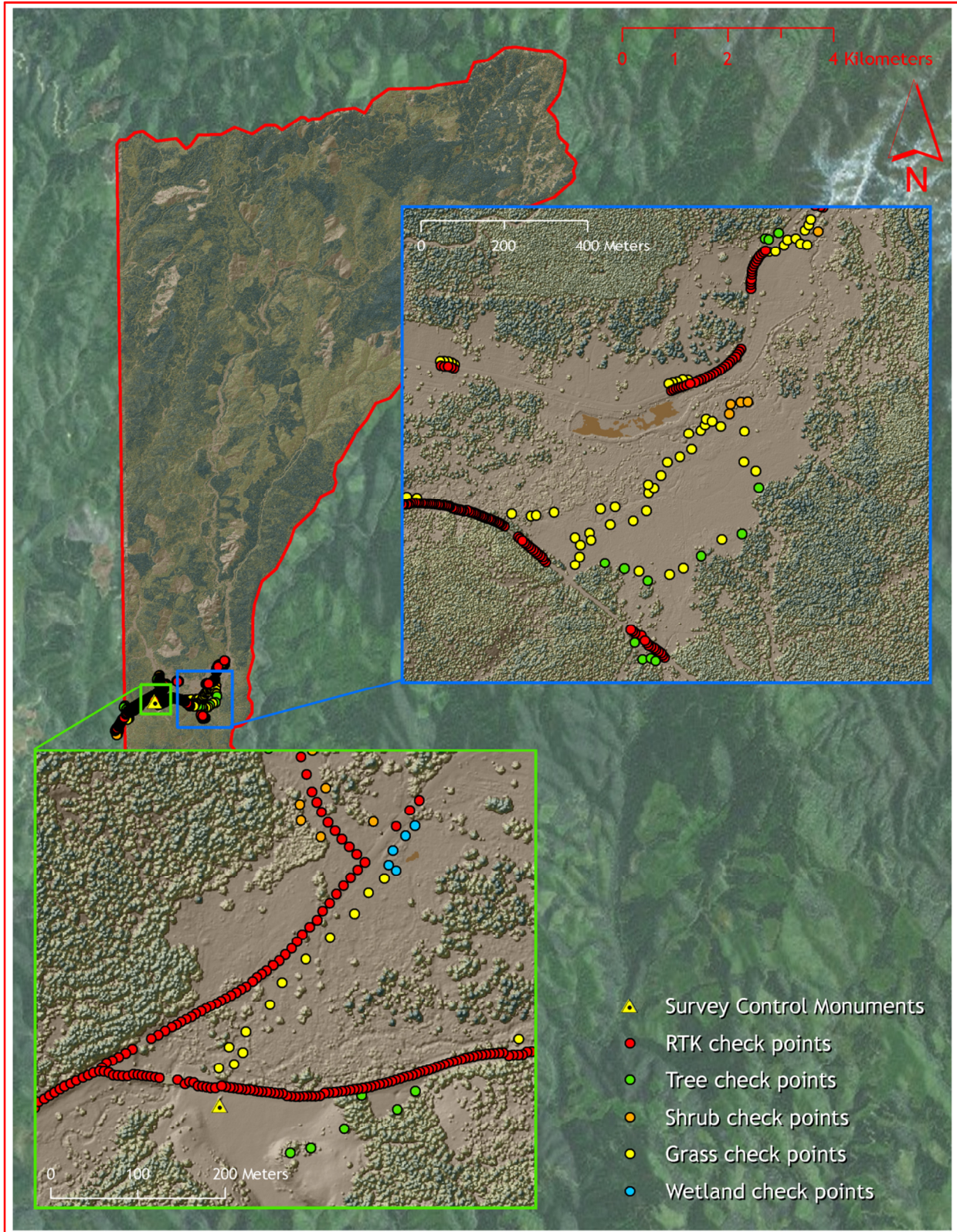


Figure 7. RTK check point, land cover check points, and control monument locations used in the Priest AOI.

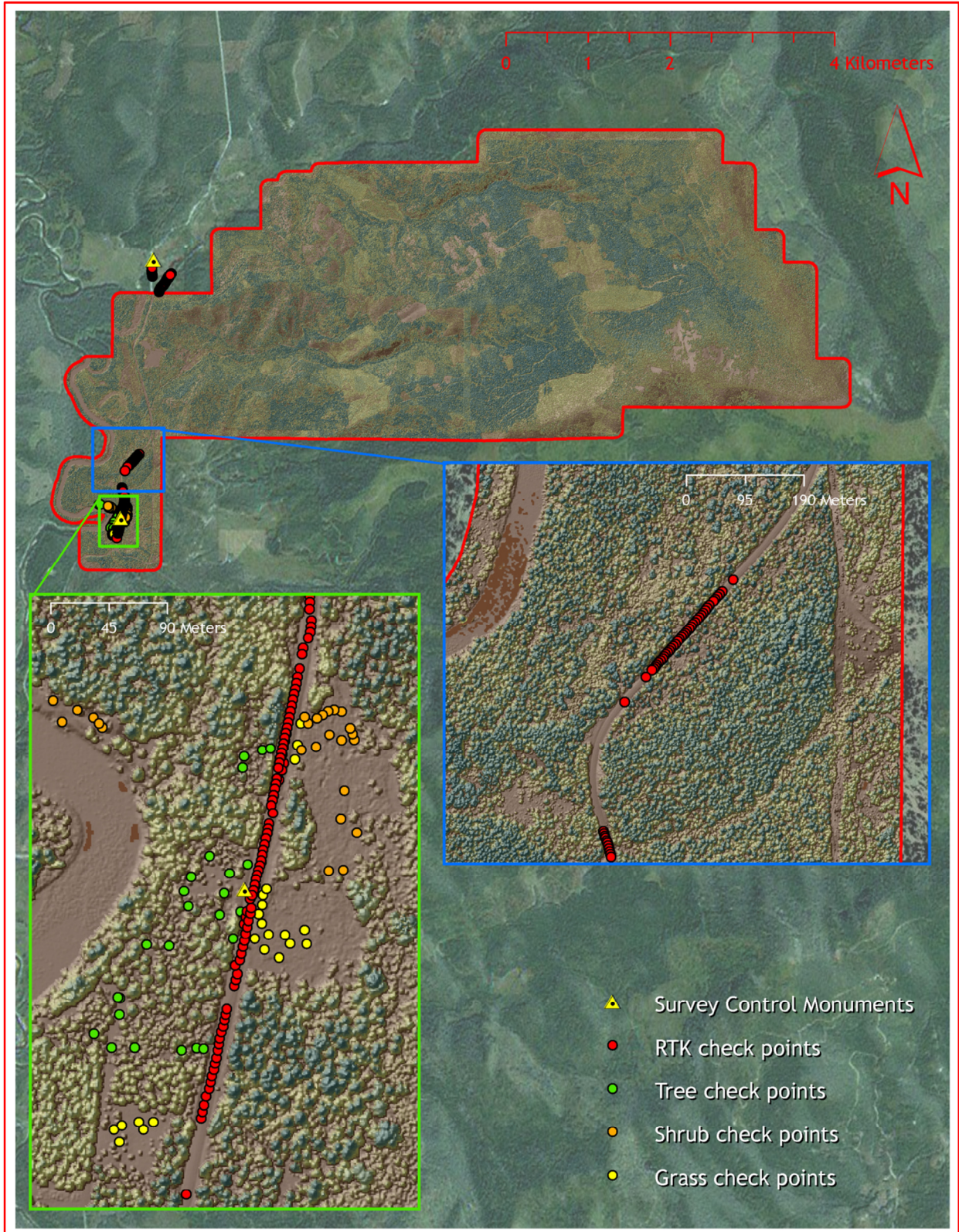
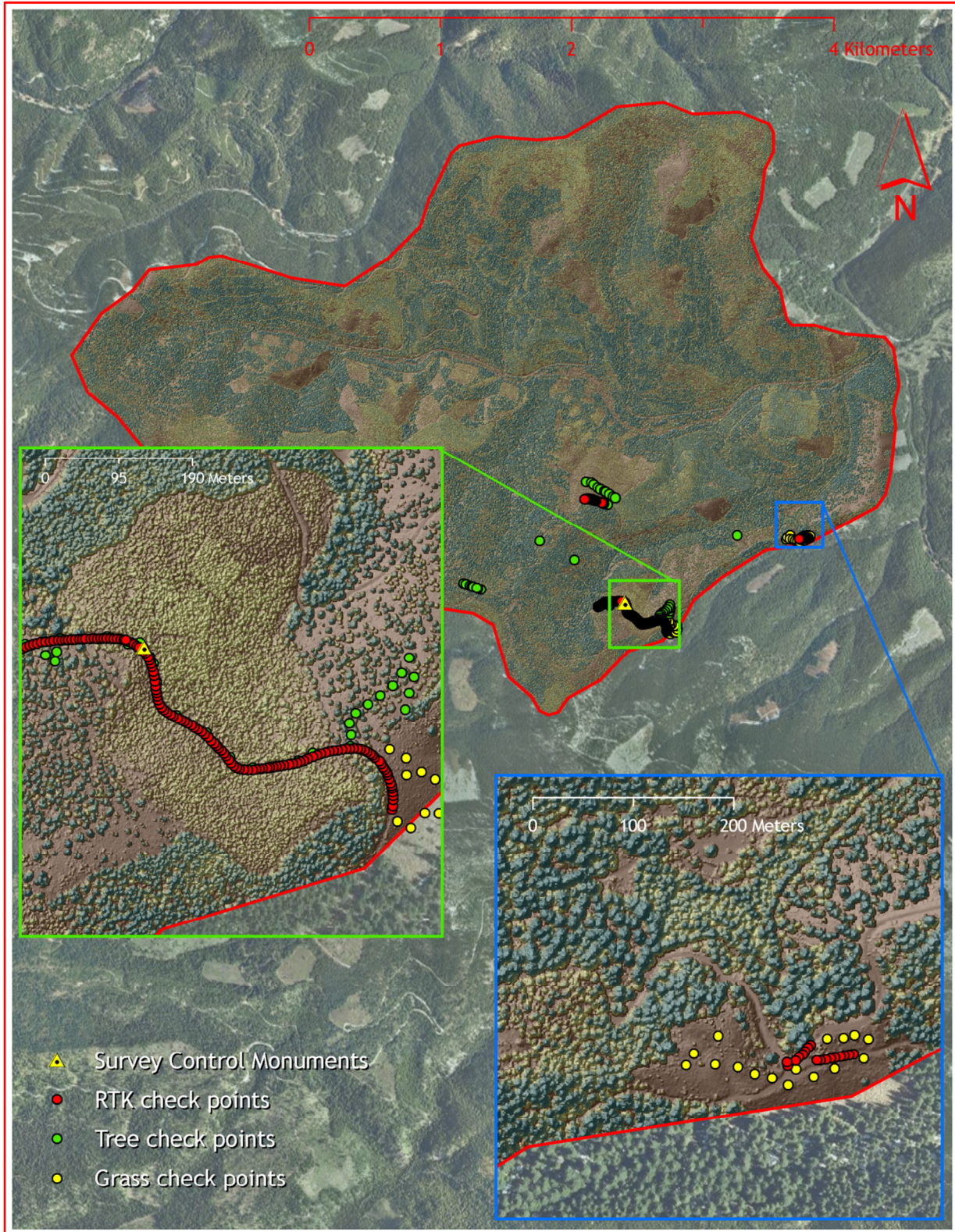


Figure 8. RTK check point, land cover check points, and control monument locations used in the Deception AOI.



3. LiDAR Data Processing

3.1 Applications and Work Flow Overview

1. Resolved kinematic corrections for aircraft position data using kinematic aircraft GPS and static ground GPS data.
Software: Waypoint GPS v.8.10, Trimble Geomatics Office v.1.62
2. Developed a smoothed best estimate of trajectory (SBET) file that blends post-processed aircraft position with attitude data. Sensor head position and attitude were calculated throughout the survey. The SBET data were used extensively for laser point processing.
Software: IPAS v.1.35
3. Calculated laser point position by associating SBET position to each laser point return time, scan angle, intensity, etc. Created raw laser point cloud data for the entire survey in *.las (ASPRS v. 1.2) format.
Software: ALS Post Processing Software v.2.70
4. Imported raw laser points into manageable blocks (less than 500 MB) to perform manual relative accuracy calibration and filter for pits/birds. Ground points were then classified for individual flight lines (to be used for relative accuracy testing and calibration).
Software: TerraScan v.11.007
5. Using ground classified points per each flight line, the relative accuracy was tested. Automated line-to-line calibrations were then performed for system attitude parameters (pitch, roll, heading), mirror flex (scale) and GPS/IMU drift. Calibrations were performed on ground classified points from paired flight lines. Every flight line was used for relative accuracy calibration.
Software: TerraMatch v.11.006
6. Position and attitude data were imported. Resulting data were classified as ground and non-ground points. Statistical absolute accuracy was assessed via direct comparisons of ground classified points to ground RTK survey data. Data were then converted to orthometric elevations (NAVD88) by applying a Geoid03 correction.
Software: TerraScan v.11.007, TerraModeler v.11.002
7. Bare Earth models were created as a triangulated surface and exported as ArcInfo ASCII grids at a 1 meter pixel resolution. Vegetation Canopy Height models (nDSM) were created for any class at 1 meter grid spacing and exported as ArcInfo ASCII grids.
Software: TerraScan v.11.007, ArcMap v. 9.3.1, TerraModeler v.11.002

3.2 Aircraft Kinematic GPS and IMU Data

LiDAR survey datasets were referenced to the 1 Hz static ground GPS data collected over pre-surveyed monuments with known coordinates. While surveying, the aircraft collected 2 Hz kinematic GPS data, and the onboard inertial measurement unit (IMU) collected 200 Hz aircraft attitude data. Waypoint GPS v.8.10 was used to process the kinematic corrections for the aircraft. The static and kinematic GPS data were then post-processed after the survey to obtain an accurate GPS solution and aircraft positions. IPAS v.1.35 was used to develop a trajectory file that includes corrected aircraft position and attitude information. The

LiDAR Data Acquisition and Processing: Clearwater, ID: Delivery 2

trajectory data for the entire flight survey session were incorporated into a final smoothed best estimated trajectory (SBET) file that contains accurate and continuous aircraft positions and attitudes.

3.3 Laser Point Processing

Laser point coordinates were computed using the IPAS and ALS Post Processor software suites based on independent data from the LiDAR system (pulse time, scan angle), and aircraft trajectory data (SBET). Laser point returns (first through fourth) were assigned an associated (x, y, z) coordinate along with unique intensity values (0-255). The data were output into large LAS v. 1.2 files with each point maintaining the corresponding scan angle, return number (echo), intensity, and x, y, z (easting, northing, and elevation) information.

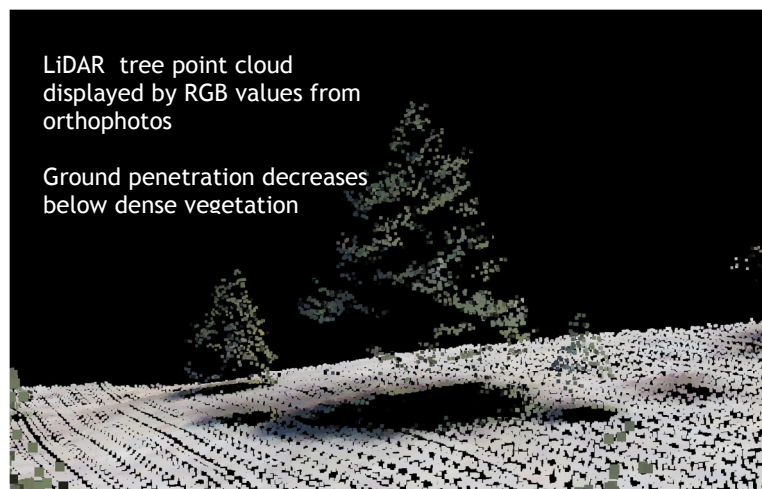
These initial laser point files were too large for subsequent processing. To facilitate laser point processing, bins (polygons) were created to divide the dataset into manageable sizes (< 500 MB). Flightlines and LiDAR data were then reviewed to ensure complete coverage of the survey area and positional accuracy of the laser points.

Laser point data were imported into processing bins in TerraScan, and manual calibration was performed to assess the system offsets for pitch, roll, heading and scale (mirror flex). Using a geometric relationship developed by Watershed Sciences, each of these offsets was resolved and corrected if necessary.

LiDAR points were then filtered for noise, pits (artificial low points), and birds (true birds as well as erroneously high points) by screening for absolute elevation limits, isolated points and height above ground. Each bin was then manually inspected for remaining pits and birds and spurious points were removed. In a bin containing approximately 7.5-9.0 million points, an average of 50-100 points are typically found to be artificially low or high. Common sources of non-terrestrial returns are clouds, birds, vapor, haze, decks, brush piles, etc.

Internal calibration was refined using TerraMatch. Points from overlapping lines were tested for internal consistency and final adjustments were made for system misalignments (i.e., pitch, roll, heading offsets and scale). Automated sensor attitude and scale corrections yielded 3-5 cm improvements in the relative accuracy. Once system misalignments were corrected, vertical GPS drift was then resolved and removed per flight line, yielding a slight improvement (<1 cm) in relative accuracy.

The TerraScan software suite is designed specifically for classifying near-ground points (Soininen, 2004). The processing sequence began by 'removing' all points that were not 'near' the earth based on geometric constraints used to evaluate multi-return points. The resulting bare earth (ground) model



was visually inspected and additional ground point modeling was performed in site-specific areas to improve ground detail. This manual editing of ground often occurs in areas with known ground modeling deficiencies, such as: bedrock outcrops, cliffs, deeply incised stream banks, and dense vegetation. In some cases, automated ground point classification erroneously included known vegetation (i.e., understory, low/dense shrubs, etc.). These points were manually reclassified. Ground surface rasters were then developed from triangulated irregular networks (TINs) of ground points.

4. LiDAR Accuracy Assessment

4.1 Laser Noise and Relative Accuracy

Laser point absolute accuracy is largely a function of laser noise and relative accuracy. To minimize these contributions to absolute error, we first performed a number of noise filtering and calibration procedures prior to evaluating absolute accuracy.

Laser Noise

For any given target, laser noise is the breadth of the data cloud per laser return (i.e., last, first, etc.). Lower intensity surfaces (roads, rooftops, still/calm water) experience higher laser noise. The laser noise range for this survey was approximately 0.02 meters.

Relative Accuracy

Relative accuracy refers to the internal consistency of the data set - the ability to place a laser point in the same location over multiple flight lines, GPS conditions, and aircraft attitudes. Affected by system attitude offsets, scale, and GPS/IMU drift, internal consistency is measured as the divergence between points from different flight lines within an overlapping area. Divergence is most apparent when flight lines are opposing. When the LiDAR system is well calibrated, the line-to-line divergence is low (<10 cm). See Appendix A for further information on sources of error and operational measures that can be taken to improve relative accuracy.

Relative Accuracy Calibration Methodology

1. **Manual System Calibration:** Calibration procedures for each mission require solving geometric relationships that relate measured swath-to-swath deviations to misalignments of system attitude parameters. Corrected scale, pitch, roll and heading offsets were calculated and applied to resolve misalignments. The raw divergence between lines was computed after the manual calibration was completed and reported for each survey area.
2. **Automated Attitude Calibration:** All data were tested and calibrated using TerraMatch automated sampling routines. Ground points were classified for each individual flight line and used for line-to-line testing. System misalignment offsets (pitch, roll and heading) and scale were solved for each individual mission and applied to respective mission datasets. The data from each mission were then blended when imported together to form the entire area of interest.
3. **Automated Z Calibration:** Ground points per line were used to calculate the vertical divergence between lines caused by vertical GPS drift. Automated Z calibration was the final step employed for relative accuracy calibration.

4.2 Absolute Accuracy

Laser point absolute accuracy is largely a function of laser noise and relative accuracy. To minimize these contributions to absolute error, a number of noise filtering and calibration procedures were performed prior to evaluating absolute accuracy. The LiDAR quality assurance process uses the data from the real-time kinematic (RTK) ground survey conducted in the AOI. For Delivery 2, a total of **1501 RTK GPS** measurements were collected on hard surfaces distributed among multiple flight swaths. Suitable and accessible hard-surfaces limited the number of RTK points able to be collected. To assess absolute accuracy the location coordinates of these known RTK ground points were compared to those calculated for the closest ground-classified laser points.

The vertical accuracy of the LiDAR data is described as the mean and standard deviation (sigma - σ) of divergence of LiDAR point coordinates from RTK ground survey point coordinates. To provide a sense of the model predictive power of the dataset, the root mean square error (RMSE) for vertical accuracy is also provided. These statistics assume the error distributions for x, y, and z are normally distributed, thus the skew and kurtosis of distributions are considered when evaluating error statistics.

Statements of statistical accuracy apply to fixed terrestrial surfaces only and may not be applied to areas of dense vegetation or steep terrain (See Appendix A).

5. Study Area Results

Summary statistics for accuracy (relative and absolute) and point resolution of the LiDAR data collected in the Clearwater, ID survey areas are presented below in terms of central tendency, variation around the mean, and the spatial distribution of the data (for point resolution by tile) per AOI.

The initial dataset, acquired to be ≥ 4 points per square meter, was filtered as described previously to remove spurious or inaccurate points. Additionally, some types of surfaces (i.e., dense vegetation, breaks in terrain, water, steep slopes) may return fewer pulses (delivered density) than the laser originally emitted (native density).

Ground classifications were derived from automated ground surface modeling and manual, supervised classifications where it was determined that the automated model had failed. Ground return densities will be lower in areas of dense vegetation, water, or buildings.

In addition to the hard surface RTK data collection, points were also collected independently on four different land cover types within in the Clearwater AOIs by Watershed Sciences. Individual accuracies were calculated for each land-cover type to assess confidence in the LiDAR derived ground models across land-cover classes.

The land cover classes for the Clearwater, ID study areas include:

- Grass
- Shrubs
- Trees
- Wetland

5.1 Data Summary: Laundry China Osier

Table 2. LiDAR Resolution and Accuracy - Specifications and Achieved Values

	Targeted	Achieved
Resolution:	≥ 4 points/m ²	5.65 points/m ²
*Vertical Accuracy (1 σ):	<15 cm	4.5 cm

5.1.1 Data Density/Resolution

Figures 11 and 12 display the distribution of average native and ground point densities for each processing bin.

LiDAR data resolution for the Laundry China Osier AOI:

- Average Point (First Return) Density = 5.65 points/m²
- Average Ground Point Density = 0.72 points/m²

Figure 9. Density distribution for first return laser points

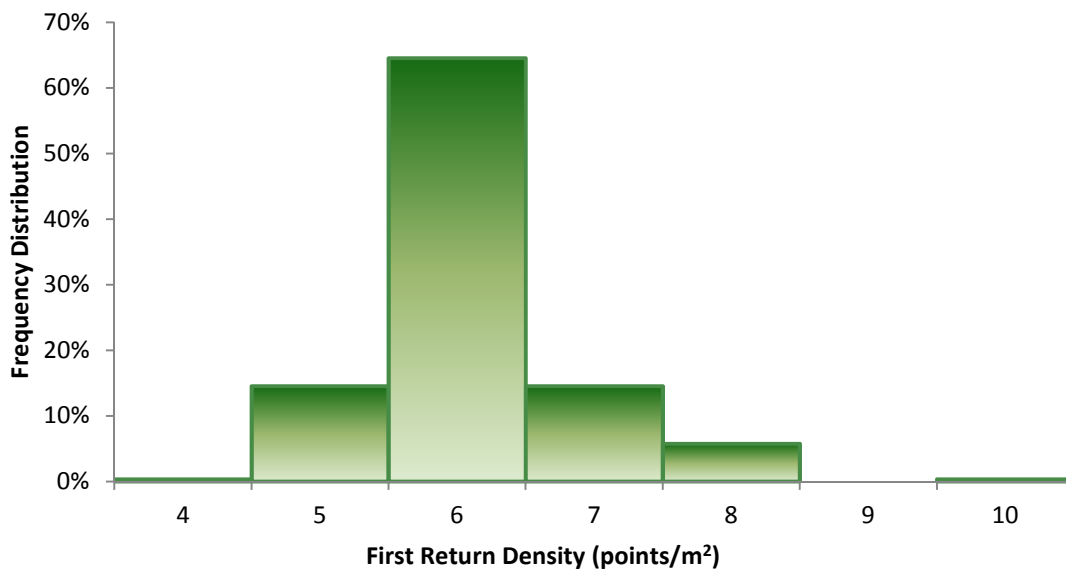


Figure 10. Density distribution for ground classified laser points

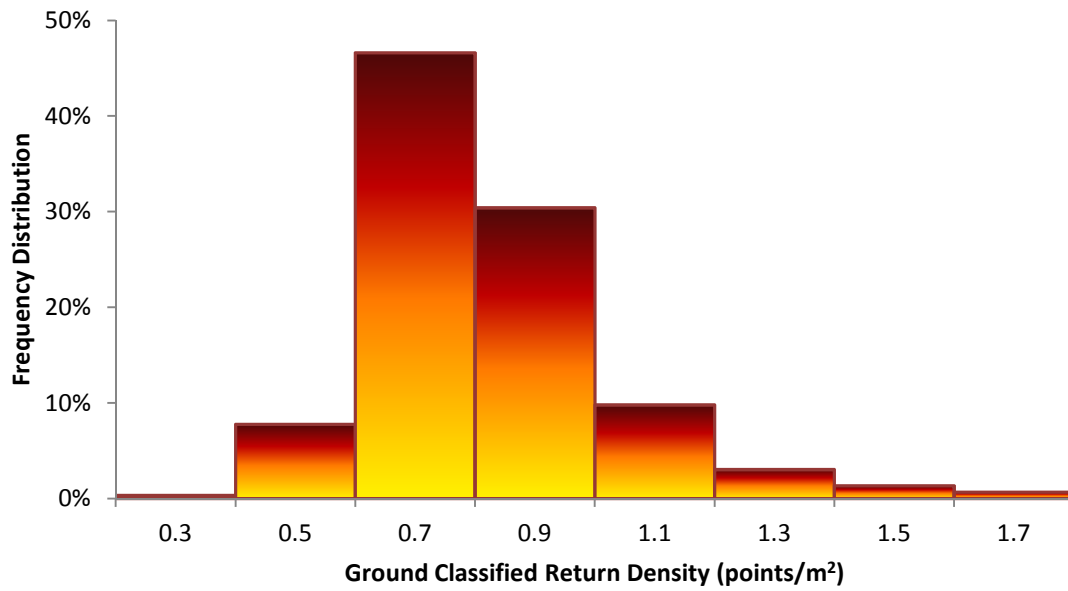


Figure 11. Density distribution map for first return points by processing bin for Laundry China Osier AOI

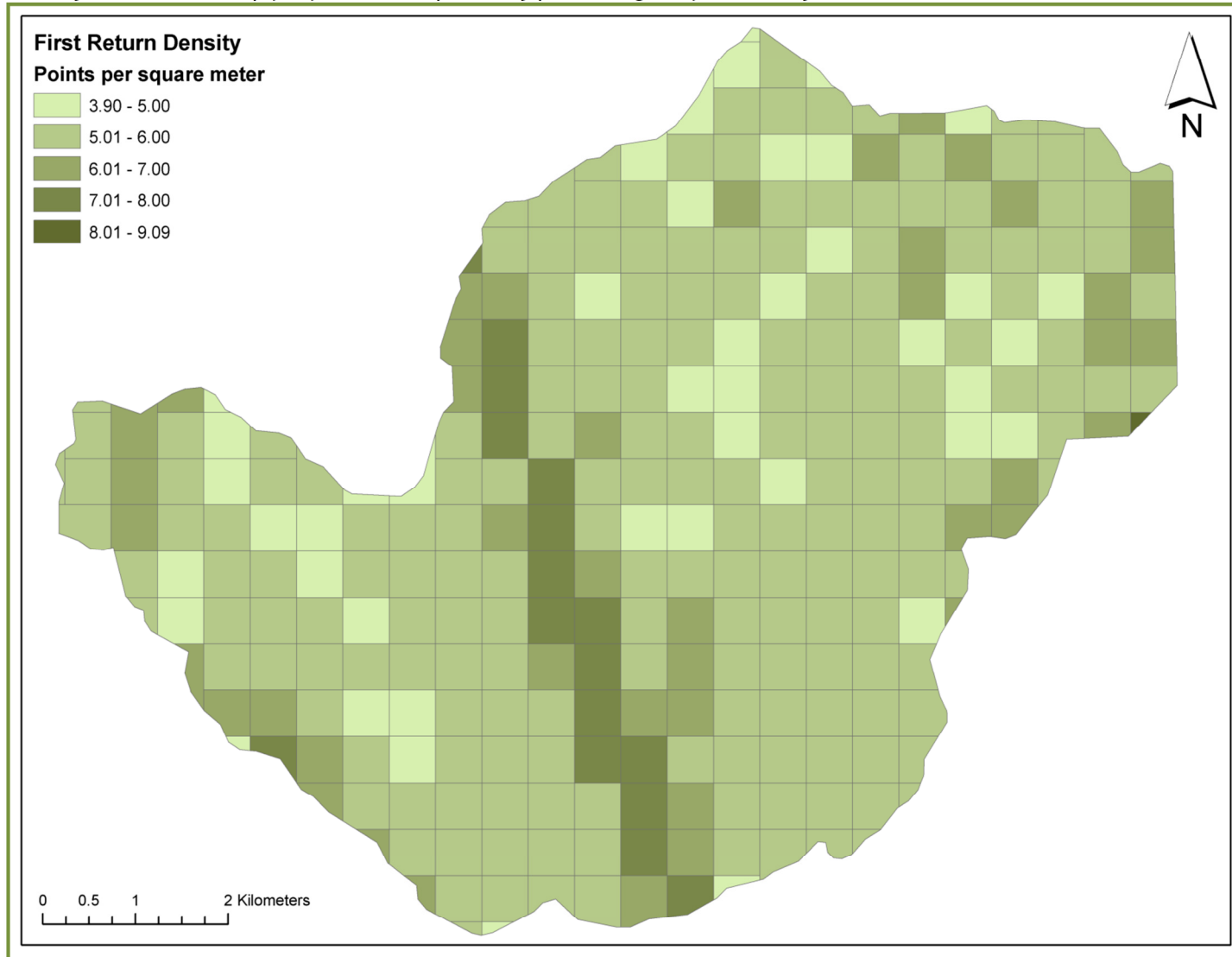
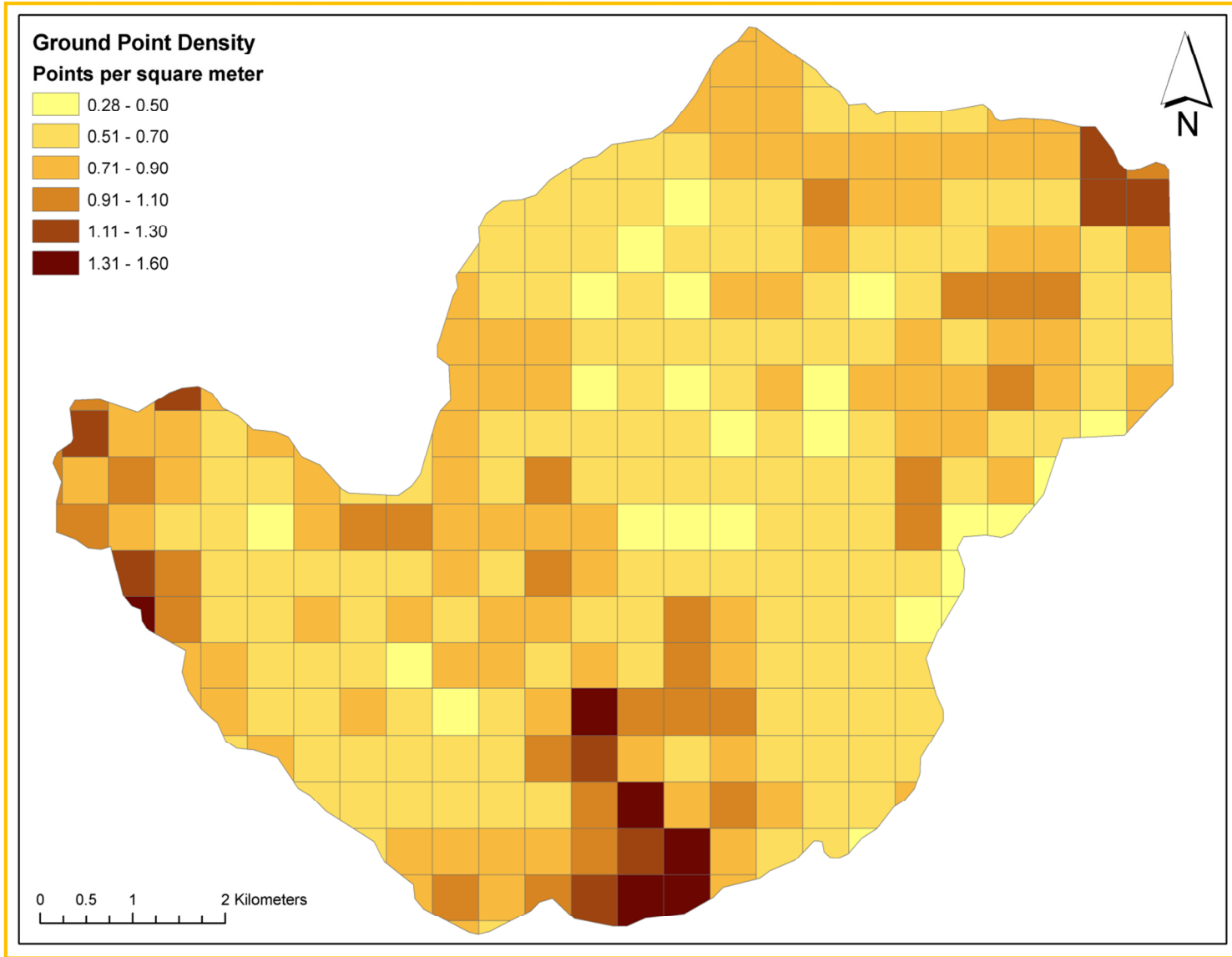


Figure 12. Density distribution map for ground return points by processing bin for Laundry China Osier AOI

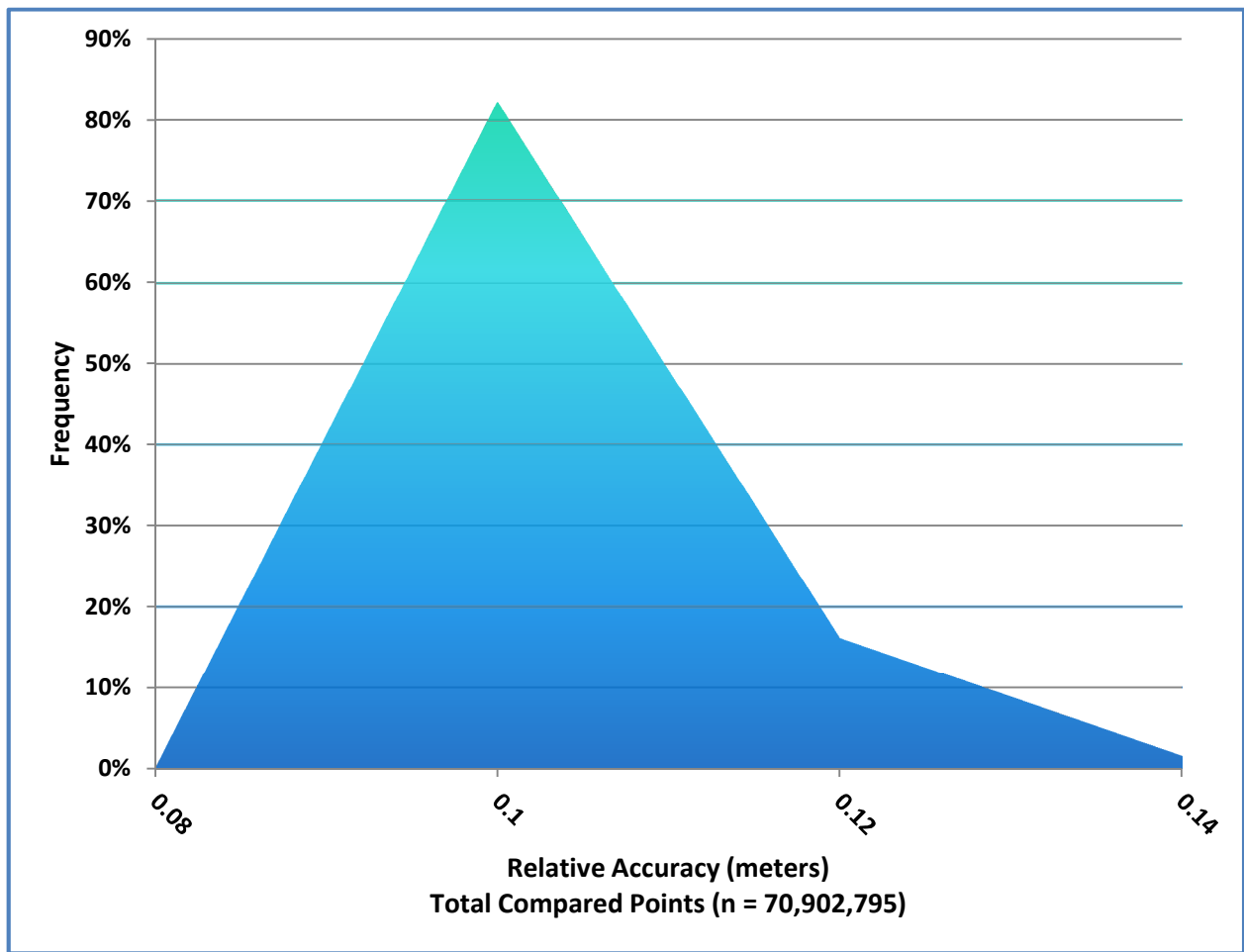


5.1.2 Relative Accuracy Calibration Results

Relative accuracy statistics for the Laundry China Osier AOI measure the full survey calibration including areas outside the delivered boundary:

- Project Average = 0.091 m
- Median Relative Accuracy = 0.090 m
- 1σ Relative Accuracy = 0.009 m
- 1.96σ Relative Accuracy = 0.019 m

Figure 13. Distribution of relative accuracies per flight line, non slope-adjusted



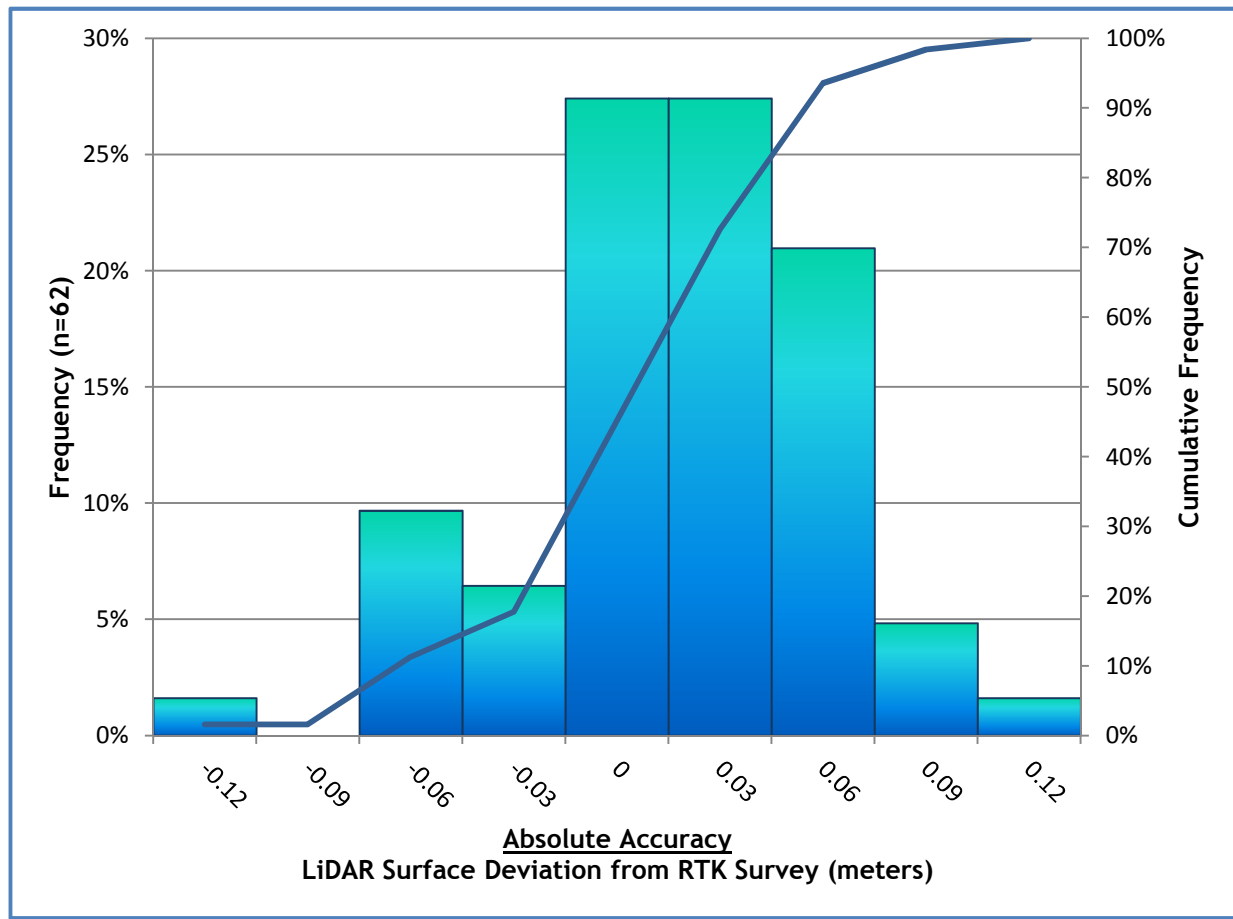
5.1.3 Absolute Accuracy

Absolute accuracies for the Laundry China Osier AOI:

Table 3. Absolute Accuracy - Deviation between laser points and RTK hard surface survey points

RTK Survey Sample Size (n): 62		
Root Mean Square Error (RMSE) = 0.045 m		Minimum Δz = -0.139 m
Standard Deviations		Maximum Δz = 0.107 m
1 sigma (σ): 0.045 m	1.96 sigma (σ): 0.089 m	Average Δz = -0.003 m

Figure 14. Absolute Accuracy - Histogram Statistics



5.1.4 Accuracy per Land Cover

Table 4. Summary of absolute accuracy statistics for each land cover type in the China AOI

Land cover	Sample size (n)	Mean Dz :	1 sigma (σ):	1.96 sigma (σ):	RMSE:
Gravel/Road	62	-0.003 m	0.045 m	0.089 m	0.045 m
Grass	27	0.028 m	0.047 m	0.093 m	0.054 m
Shrubs	27	0.054 m	0.148 m	0.290 m	0.155 m
Trees	22	0.111 m	0.094 m	0.185 m	0.144 m



5.2 Data Summary: Walde Pete King

Table 5. LiDAR Resolution and Accuracy - Specifications and Achieved Values

	Targeted	Achieved
Resolution:	≥ 4 points/m ²	6.81 points/m ²
*Vertical Accuracy (1 σ):	<15 cm	3.2 cm

5.2.1 Data Density/Resolution

Figures 17 and 18 display the distribution of average native and ground point densities for each processing bin.

LiDAR data resolution for the Walde Pete King AOI:

- Average Point (First Return) Density = 6.81 points/m²
- Average Ground Point Density = 0.53 points/m²

Figure 15. Density distribution for first return laser points

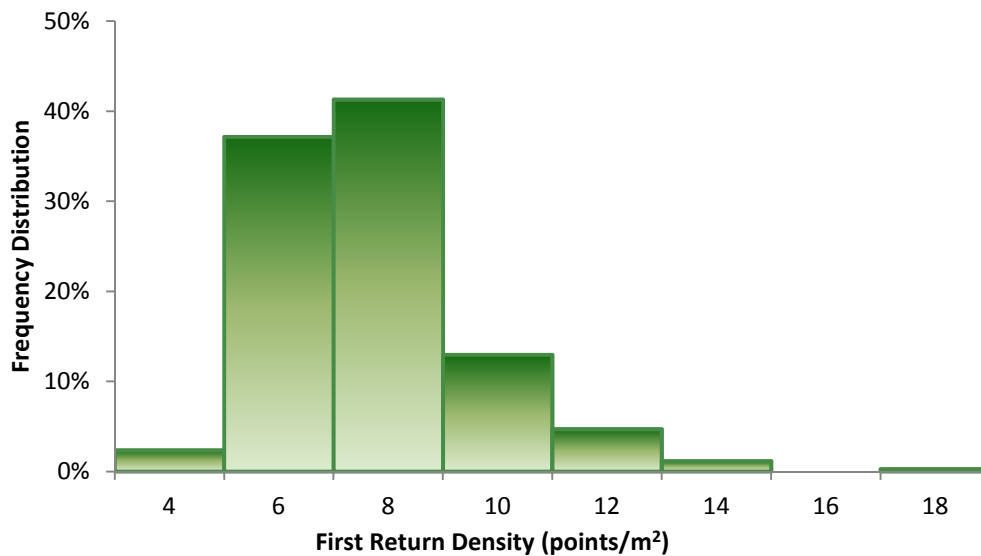


Figure 16. Density distribution for ground classified laser points

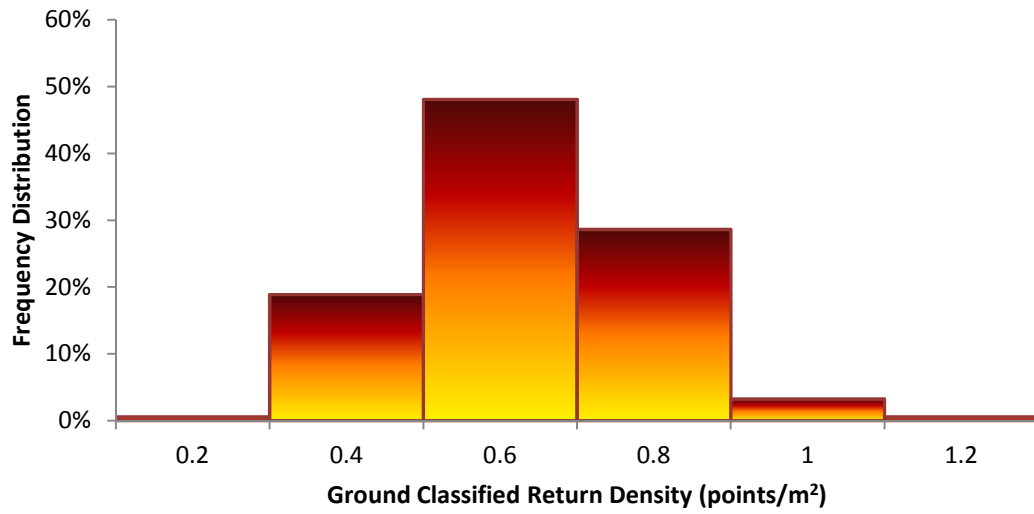


Figure 17. Density distribution map for first return points by processing bin for the Walde Pete King AOI

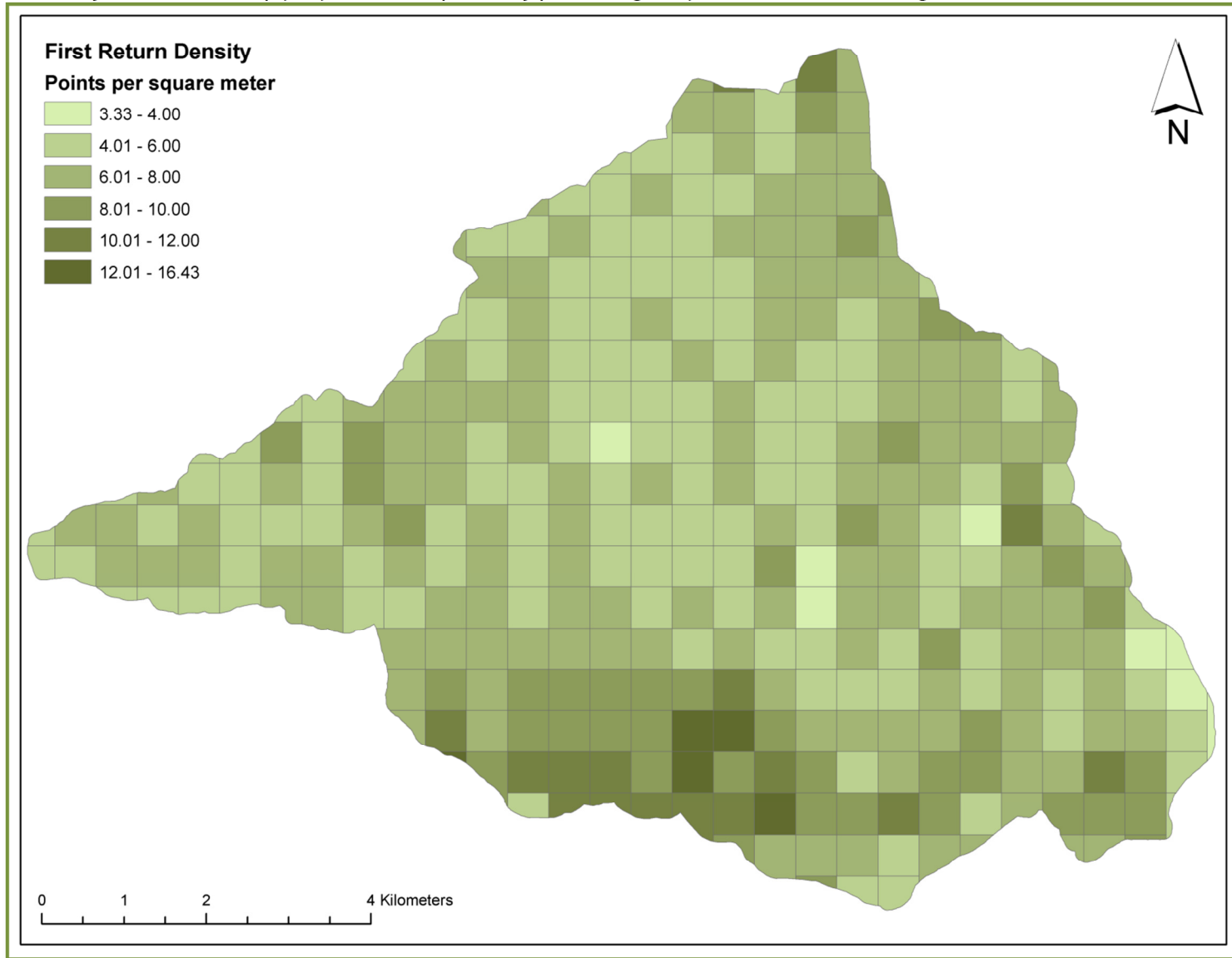
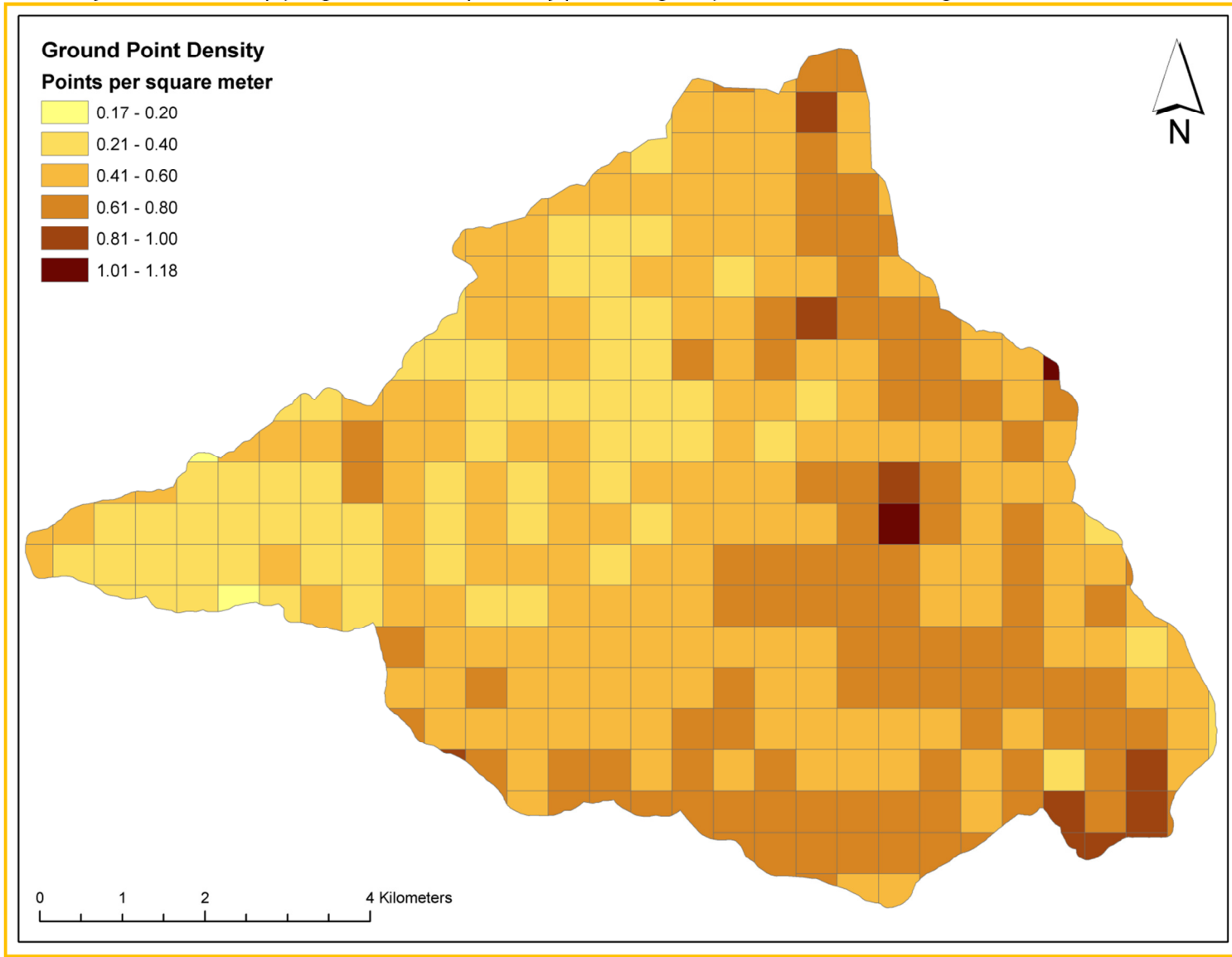


Figure 18. Density distribution map for ground return points by processing bin for the Walde Pete King AOI

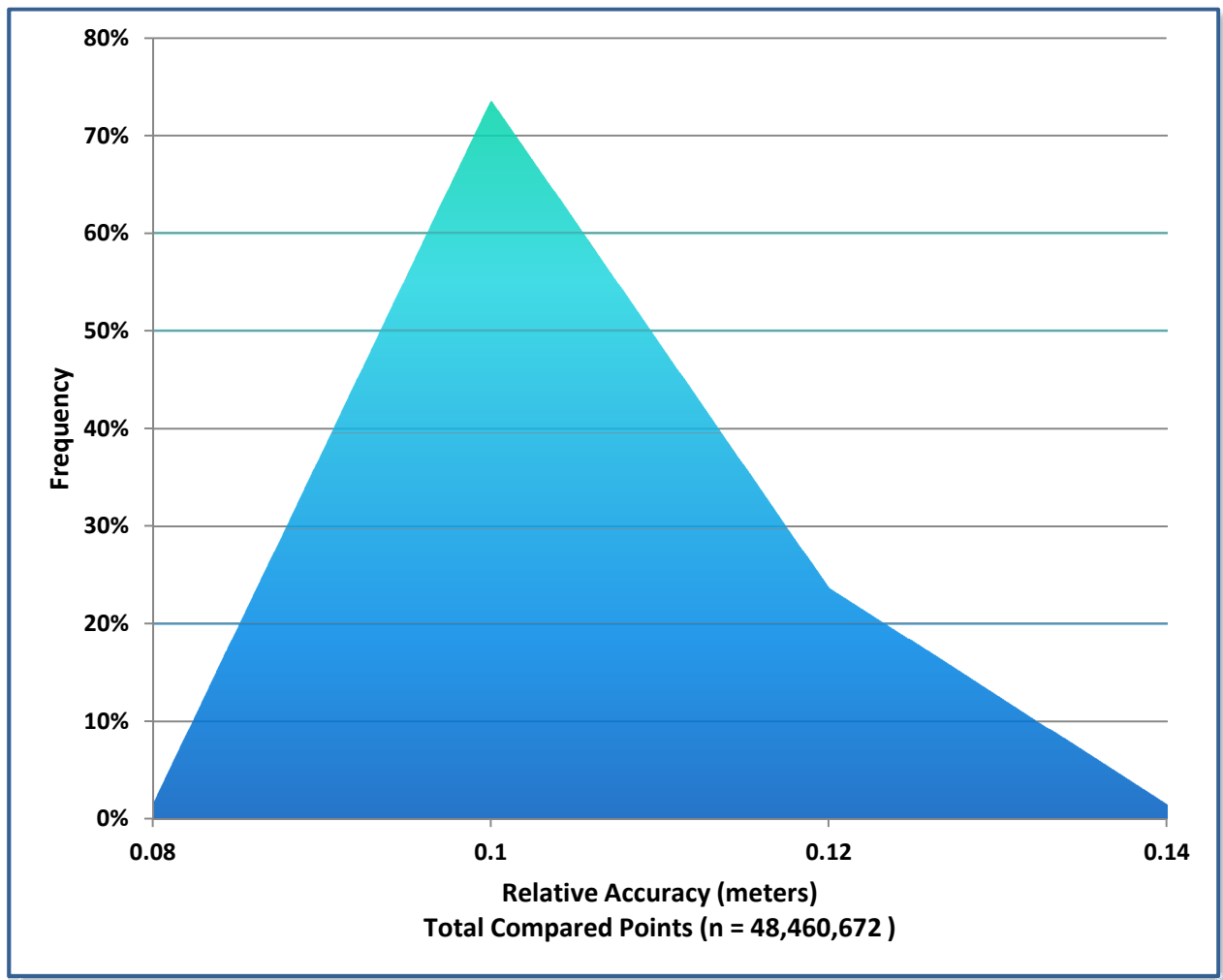


5.2.2 Relative Accuracy Calibration Results

Relative accuracy statistics for the Walde Pete King AOI measure the full survey calibration including areas outside the delivered boundary:

- Project Average = 0.093 m
- Median Relative Accuracy = 0.093 m
- 1σ Relative Accuracy = 0.010 m
- 1.96σ Relative Accuracy = 0.019 m

Figure 19. Distribution of relative accuracies per flight line, non slope-adjusted



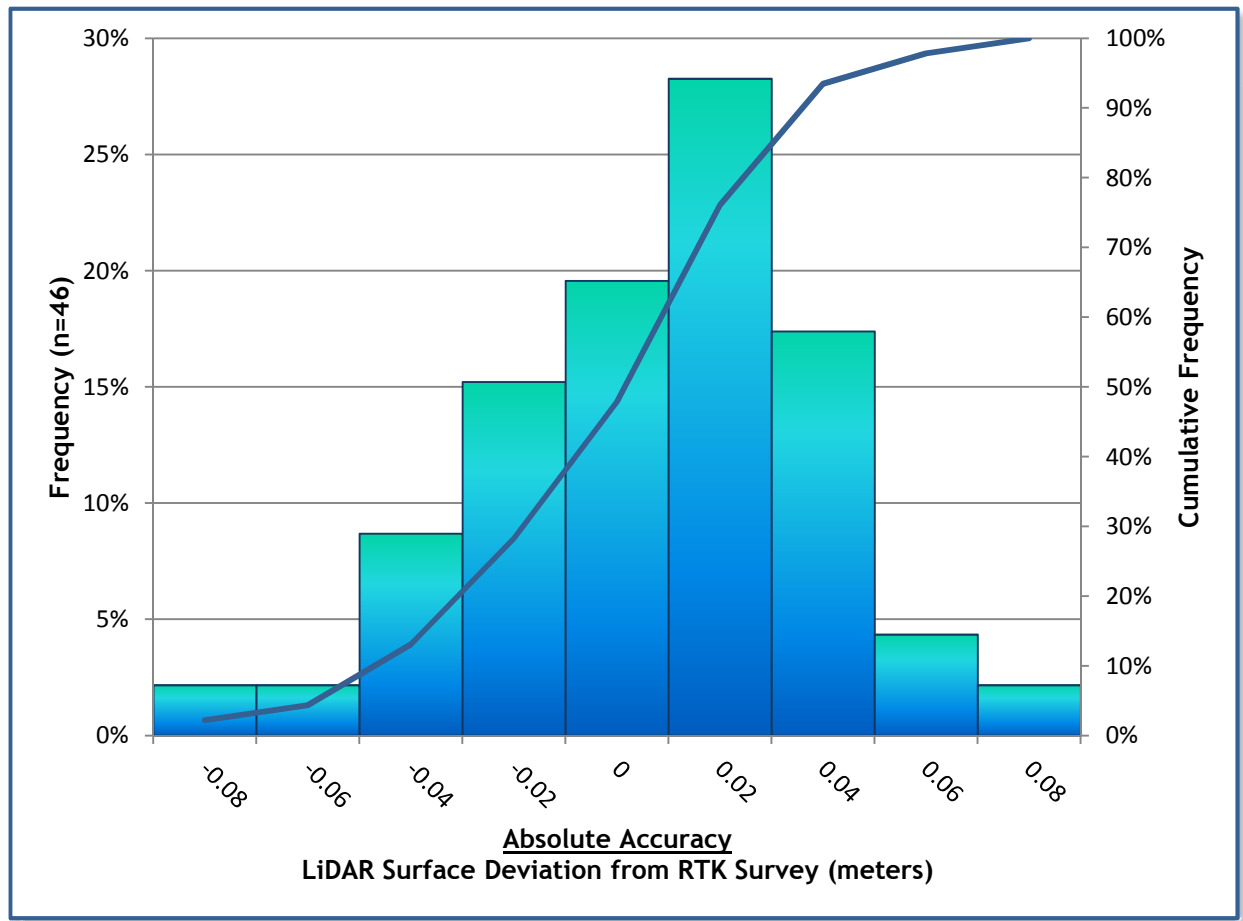
5.2.3 Absolute Accuracy

Absolute accuracies for the Walde Pete King AOI:

Table 6. Absolute Accuracy - Deviation between laser points and RTK hard surface survey points

RTK Survey Sample Size (n): 46		
Root Mean Square Error (RMSE) = 0.032 m		Minimum Δz = -0.087 m
Standard Deviations		Maximum Δz = 0.071 m
1 sigma (σ): 0.032 m	1.96 sigma (σ): 0.063 m	Average Δz = -0.001 m

Figure 20. Absolute Accuracy - Histogram Statistics



5.2.4 Accuracy per Land Cover

Table 7. Summary of absolute accuracy statistics for each land cover type in Walde Pete King AOI

Land cover	Sample size (n)	Mean Dz :	1 sigma (σ):	1.96 sigma (σ):	RMSE:
Gravel/Road	46	-0.001 m	0.032 m	0.063 m	0.032 m
Grass	25	0.081 m	0.057 m	0.111 m	0.098 m
Shrubs	24	0.146 m	0.123 m	0.242 m	0.185 m
Trees	27	0.064 m	0.150 m	0.294 m	0.160 m

5.3 Data Summary: Upper Elk

Table 8. LiDAR Resolution and Accuracy - Specifications and Achieved Values

	Targeted	Achieved
Resolution:	≥ 4 points/m ²	8.02 points/m ²
*Vertical Accuracy (1 σ):	<15 cm	3.4 cm

5.3.1 Data Density/Resolution

Figures 23 and 24 display the distribution of average native and ground point densities for each processing bin.

LiDAR data resolution for the Upper Elk AOI:

- Average Point (First Return) Density = 8.02 points/m²
- Average Ground Point Density = 0.71 points/m²

Figure 21. Density distribution for first return laser points

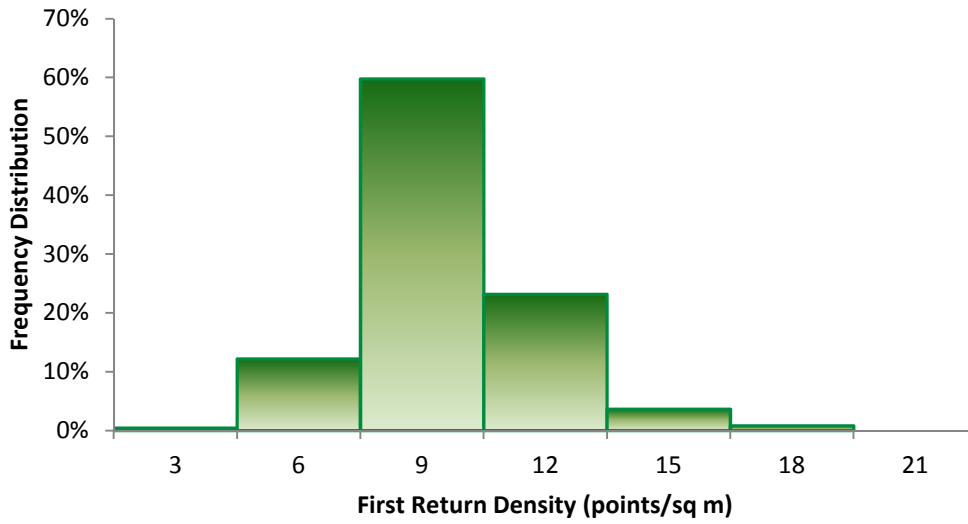


Figure 22. Density distribution for ground classified laser points

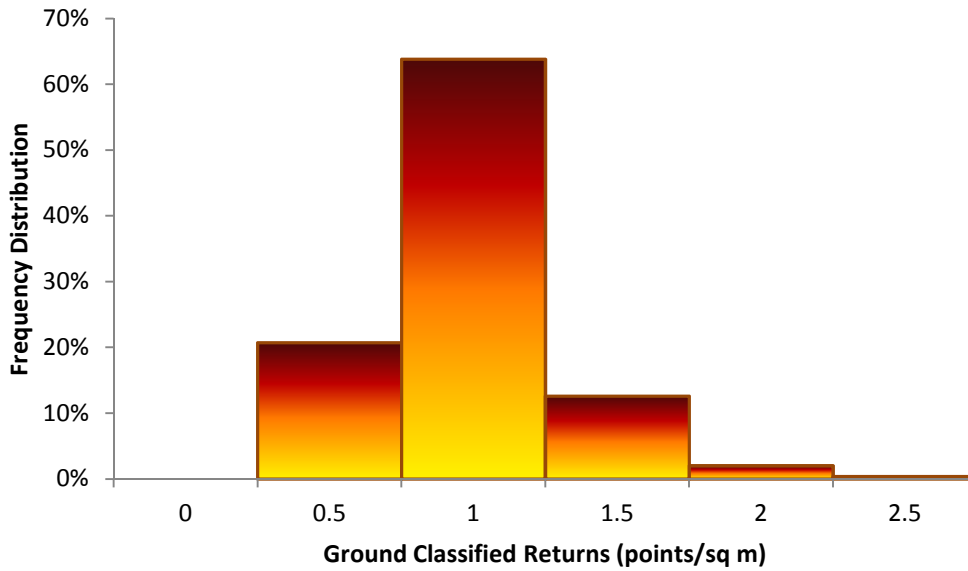


Figure 23. Density distribution map for first return points by processing bin for the Upper Elk AOI

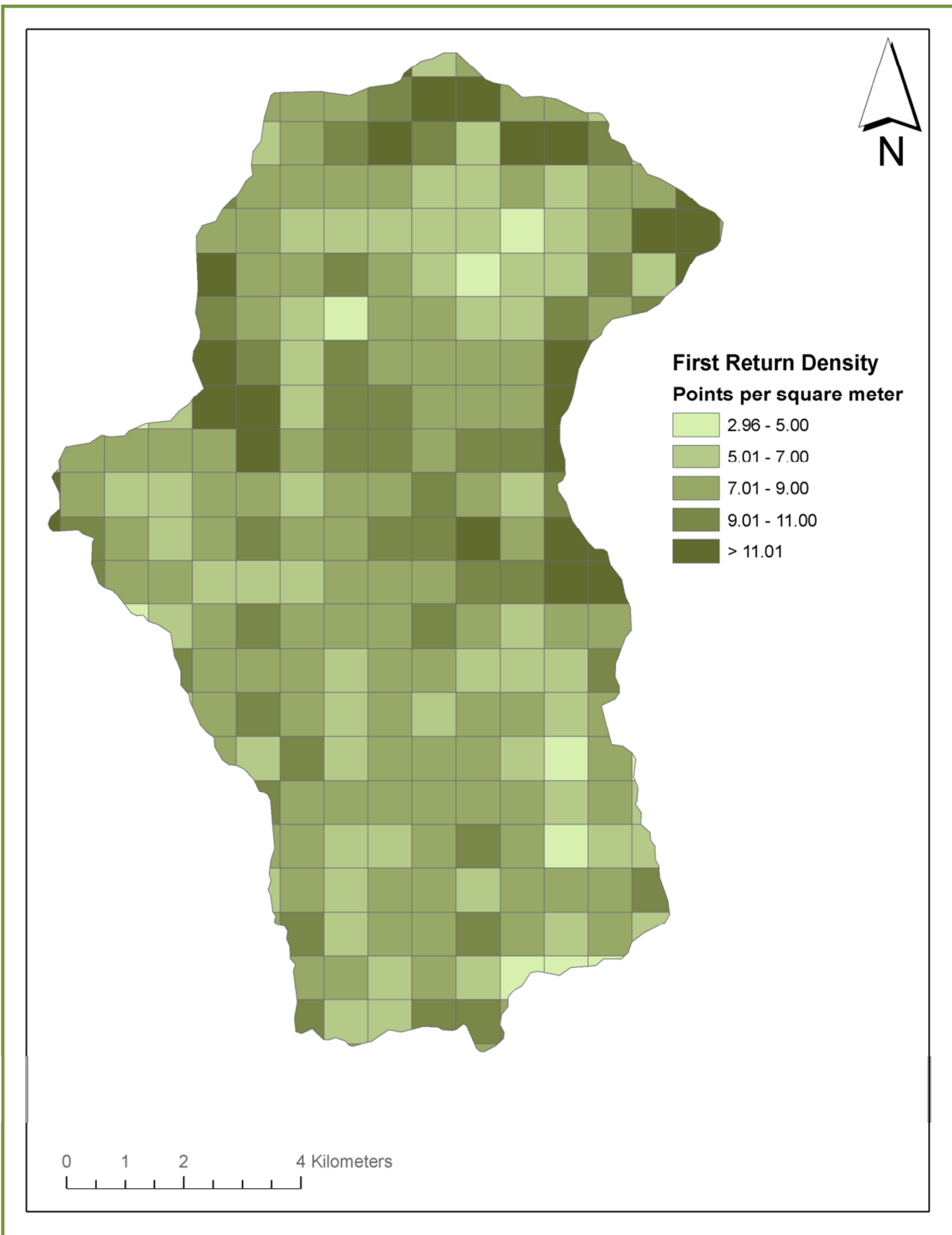
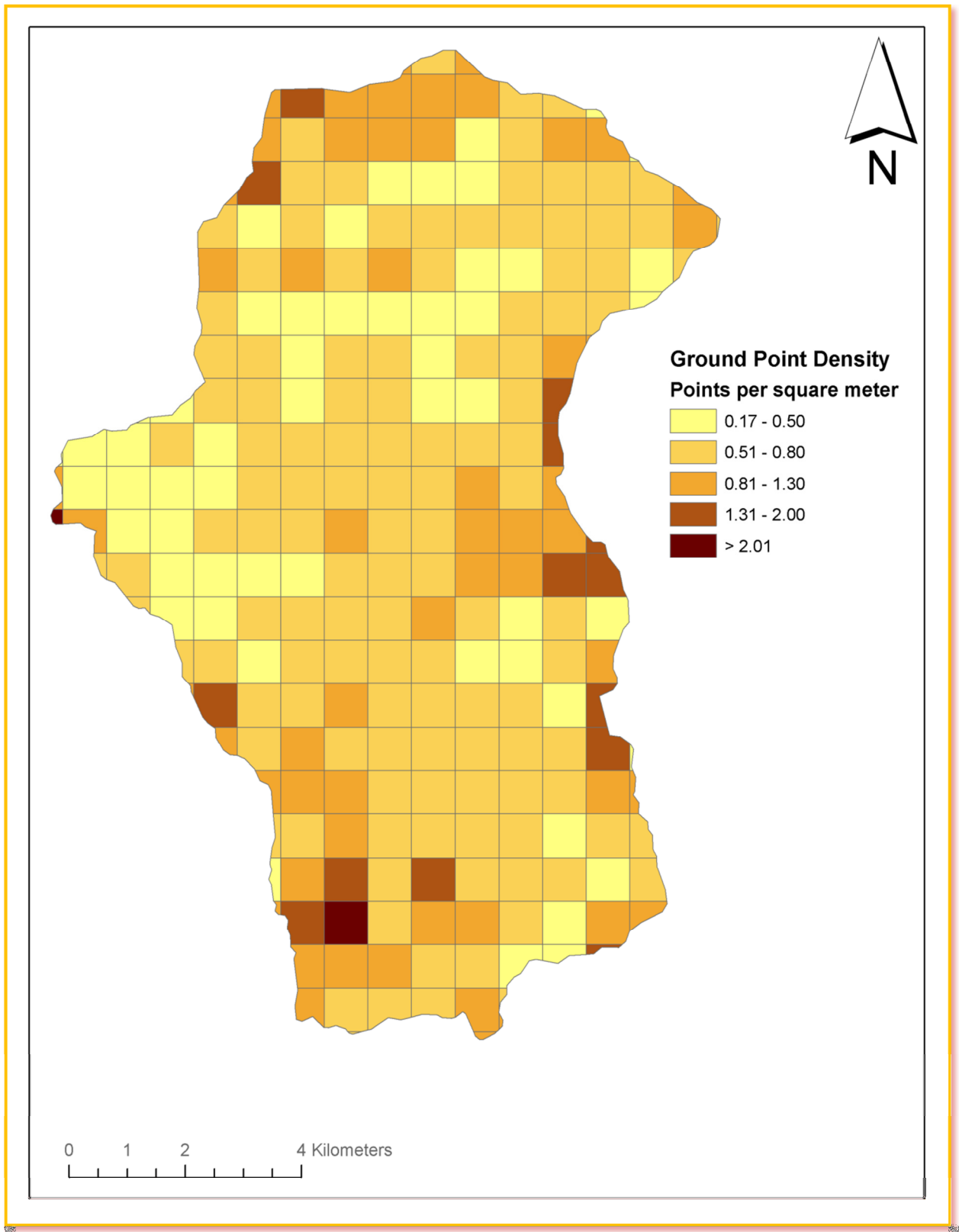


Figure 24. Density distribution map for ground return points by processing bin for the Upper Elk AOI

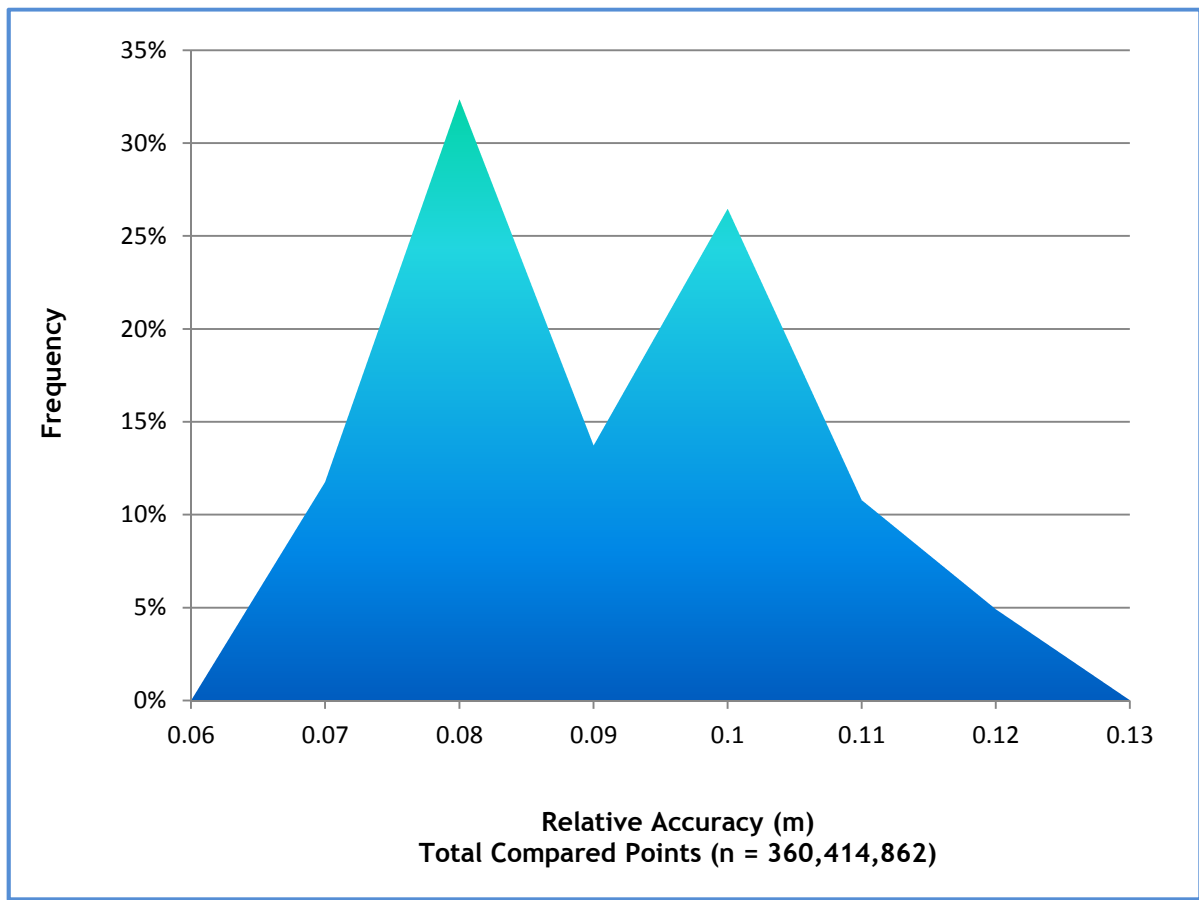


5.3.2 Relative Accuracy Calibration Results

Relative accuracy statistics for the Upper Elk AOI measure the full survey calibration including areas outside the delivered boundary:

- Project Average = 0.084 m
- Median Relative Accuracy = 0.085 m
- 1σ Relative Accuracy = 0.014 m
- 1.96σ Relative Accuracy = 0.028 m

Figure 25. Distribution of relative accuracies per flight line, non slope-adjusted



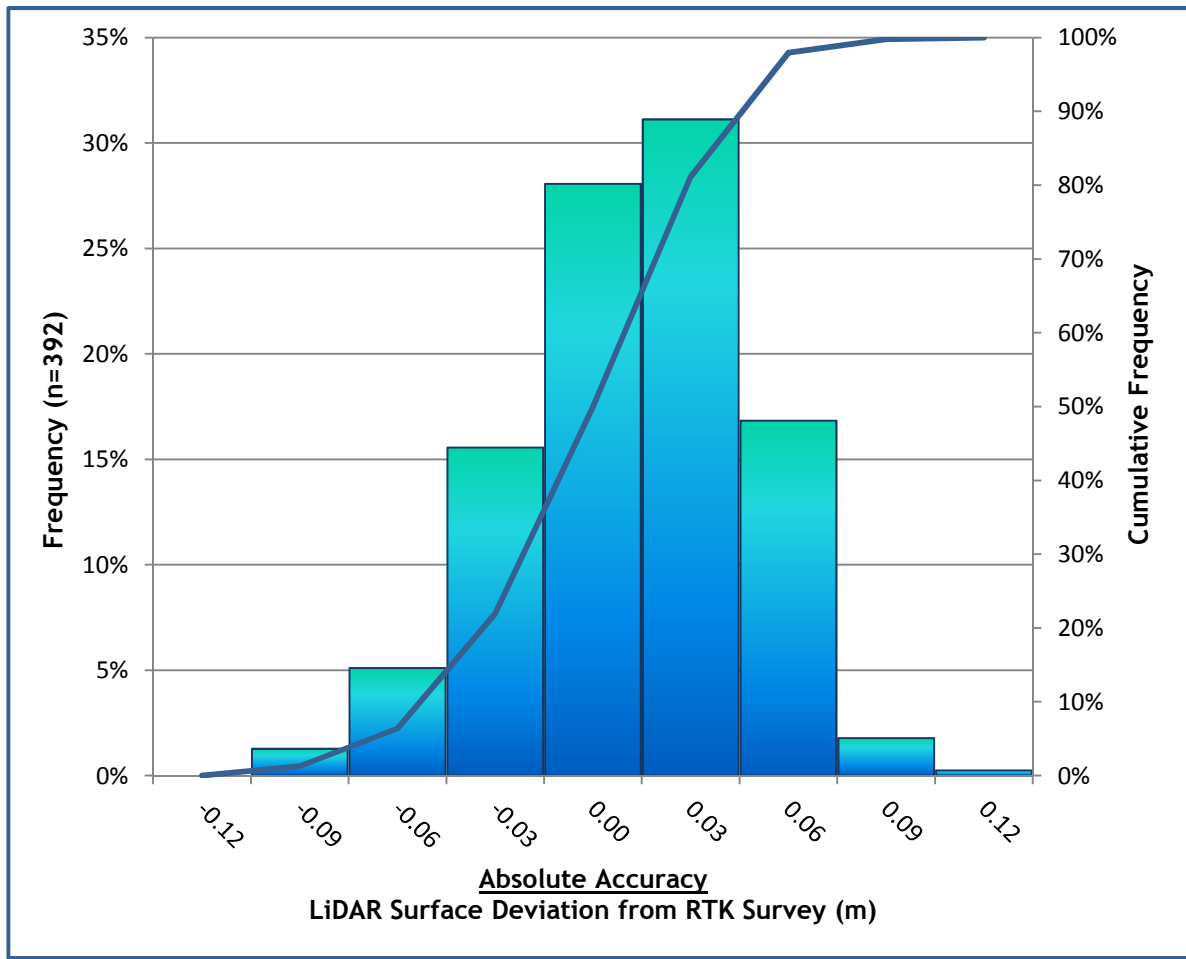
5.3.3 Absolute Accuracy

Absolute accuracies for the Upper Elk AOI:

Table 9. Absolute Accuracy - Deviation between laser points and RTK hard surface survey points

RTK Survey Sample Size (n): 392	
Root Mean Square Error (RMSE) = 0.035 m	Minimum Δz = -0.112 m
Standard Deviations 1 sigma (σ): 0.035 m 1.96 sigma (σ): 0.069 m	Maximum Δz = 0.100 m
	Average Δz = -0.002 m

Figure 26. Absolute Accuracy - Histogram Statistics



5.3.4 Accuracy per Land Cover

Table 10. Summary of absolute accuracy statistics for each land cover type in the Upper Elk AOI

Land cover	Sample size (n)	Mean Dz :	1 sigma (σ):	1.96 sigma (σ):	RMSE:
Gravel/Road	392	-0.002 m	0.035 m	0.069 m	0.035 m
Grass	53	0.209 m	0.144 m	0.282 m	0.253 m
Shrubs	24	0.265 m	0.160 m	0.315 m	0.308 m
Trees	42	0.062 m	0.093 m	0.182 m	0.017 m
Wetland	23	0.332 m	0.143 m	0.280 m	0.075 m

5.4 Data Summary: Potlatch

Table 11. LiDAR Resolution and Accuracy - Specifications and Achieved Values

	Targeted	Achieved
Resolution:	≥ 4 points/m ²	8.32 points/m ²
*Vertical Accuracy (1 σ):	<15 cm	4.0 cm

5.4.1 Data Density/Resolution

Figure 29 displays the distribution of average native and ground point densities for each processing bin.

LiDAR data resolution for the Potlatch AOI:

- Average Point (First Return) Density = 8.32 points/m²
- Average Ground Point Density = 1.09 points/m²

Figure 27. Density distribution for first return laser points

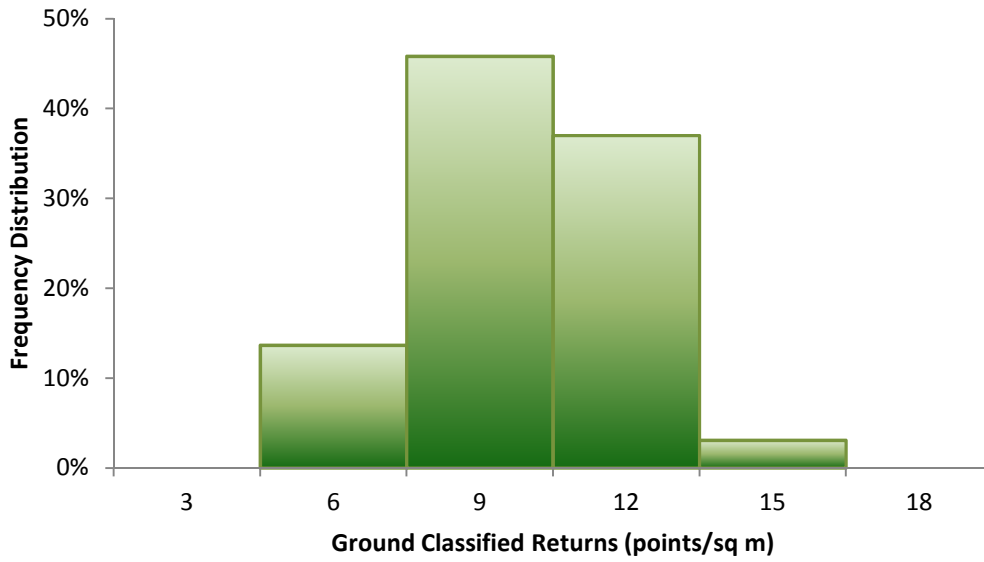


Figure 28. Density distribution for ground classified laser points

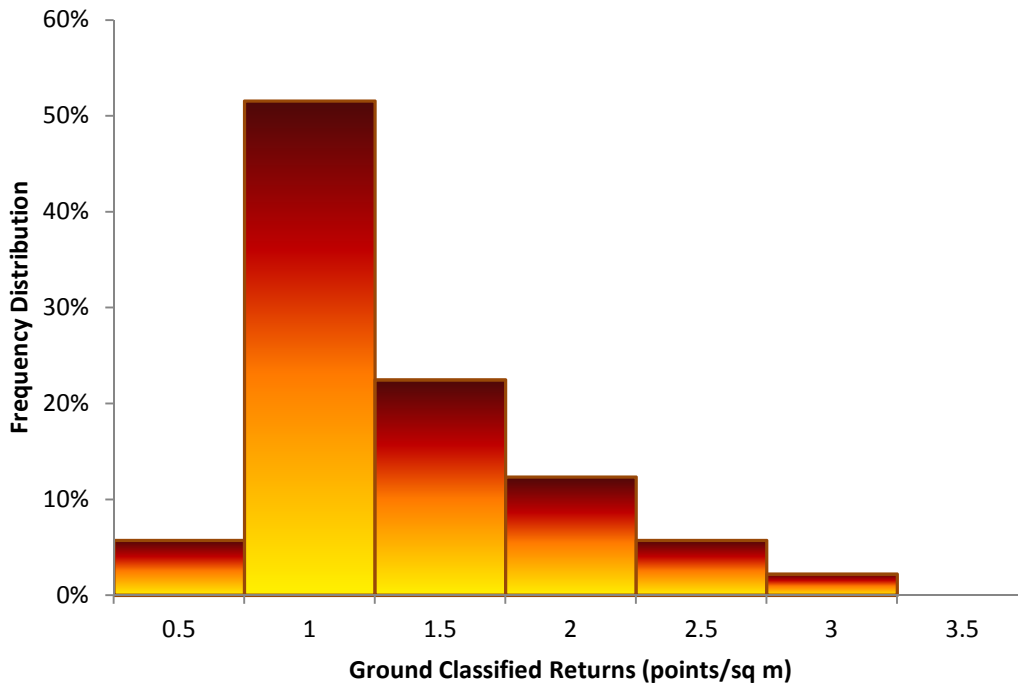
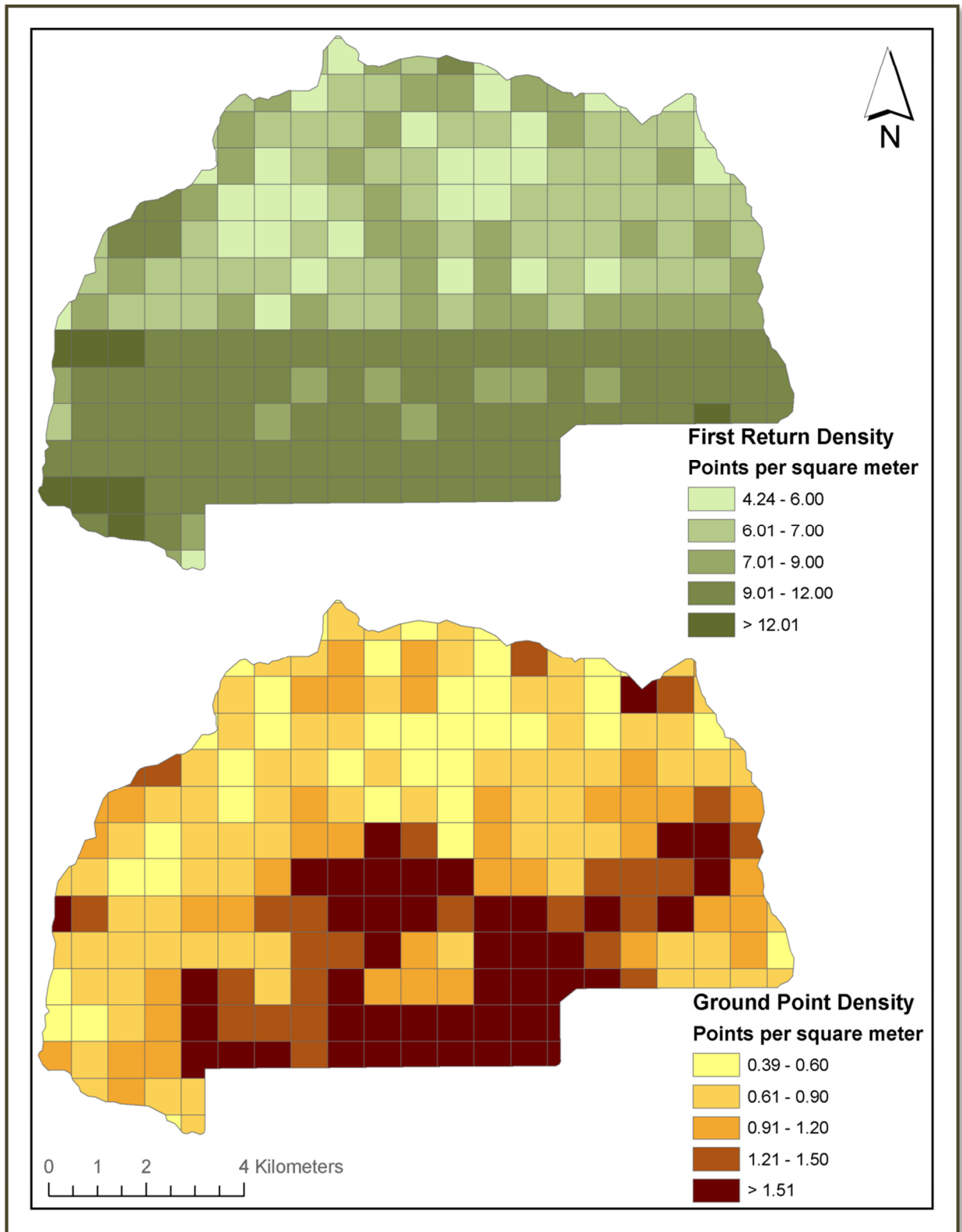


Figure 29. Density distribution map for first return points by processing bin for the Potlatch AOI

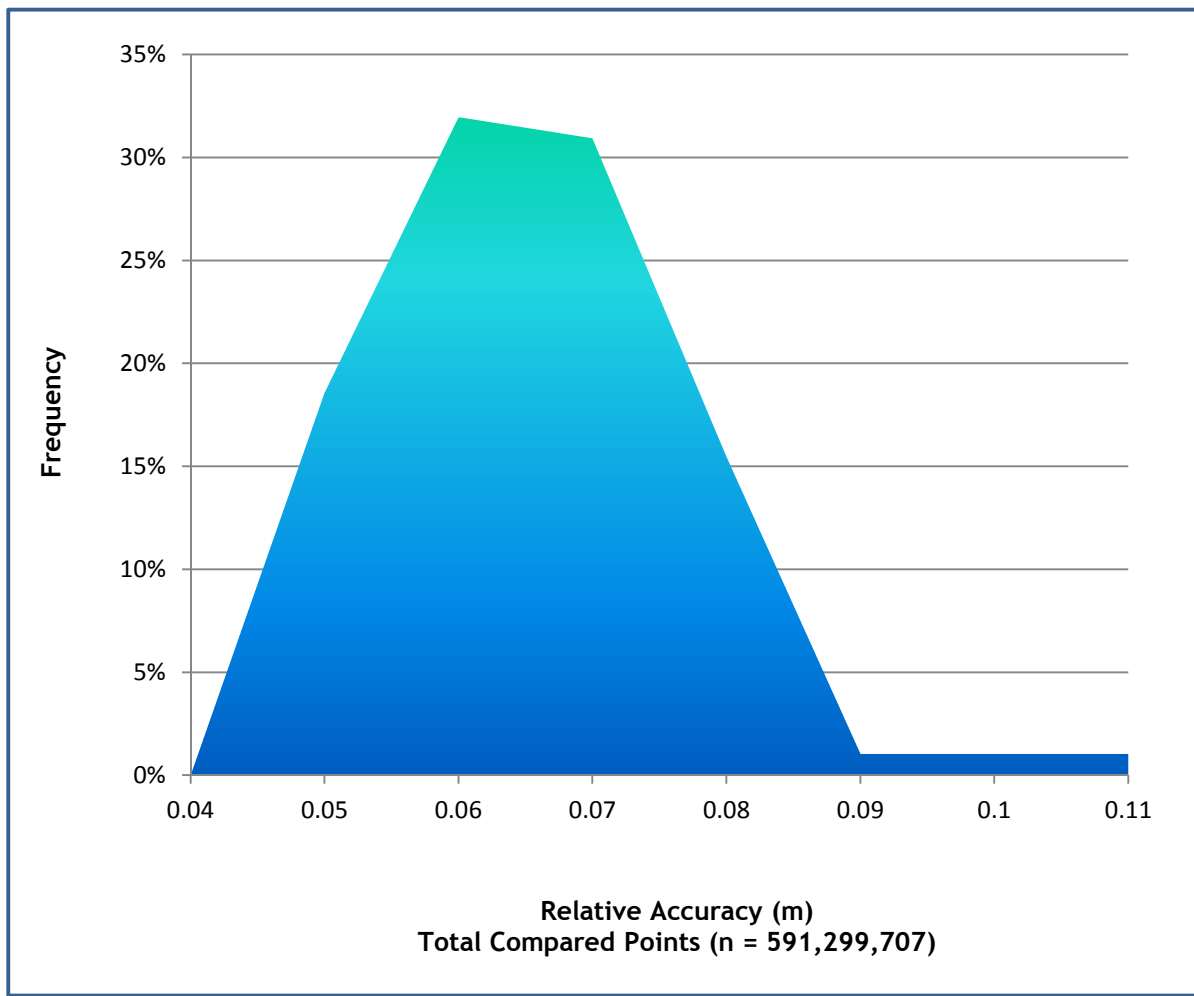


5.4.2 Relative Accuracy Calibration Results

Relative accuracy statistics for the Potlatch AOI measure the full survey calibration including areas outside the delivered boundary:

- Project Average = 0.055 m
- Median Relative Accuracy = 0.060 m
- 1σ Relative Accuracy = 0.011 m
- 1.96σ Relative Accuracy = 0.021 m

Figure 30. Distribution of relative accuracies per flight line, non slope-adjusted



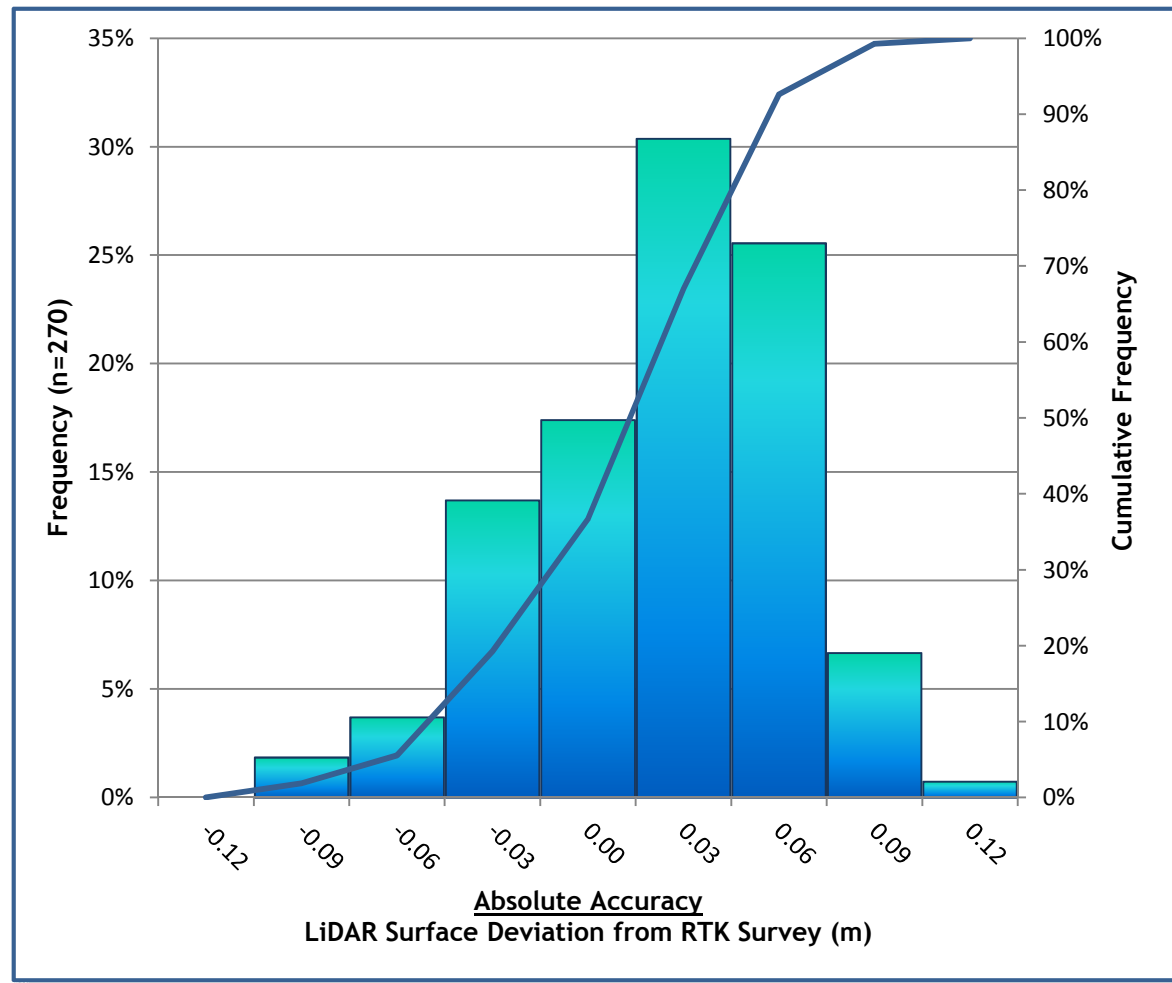
5.4.3 Absolute Accuracy

Absolute accuracies for the Potlatch AOI:

Table 12. Absolute Accuracy - Deviation between laser points and RTK hard surface survey points

RTK Survey Sample Size (n): 270	
Root Mean Square Error (RMSE) = 0.041 m	Minimum Δz = -0.109 m
Standard Deviations 1 sigma (σ): 0.040 m 1.96 sigma (σ): 0.078 m	Maximum Δz = 0.103 m
	Average Δz = 0.009 m

Figure 31. Absolute Accuracy - Histogram Statistics



5.4.4 Accuracy per Land Cover

Table 13. Summary of absolute accuracy statistics for each land cover type in the Potlatch AOI

Land cover	Sample size (n)	Mean Dz :	1 sigma (σ):	1.96 sigma (σ):	RMSE:
Gravel/Road	270	0.009 m	0.040 m	0.078 m	0.041 m
Grass	61	0.142 m	0.108 m	0.211 m	0.178 m
Shrubs	51	0.249 m	0.152 m	0.297 m	0.291 m
Trees	13	0.181 m	0.053 m	0.104 m	0.188 m

5.5 Data Summary: Musselshell

Table 14. LiDAR Resolution and Accuracy - Specifications and Achieved Values

	Targeted	Achieved
Resolution:	≥ 4 points/m ²	6.93 points/m ²
*Vertical Accuracy (1 σ):	<15 cm	3.6 cm

5.5.1 Data Density/Resolution

Figure 34 displays the distribution of average native and ground point densities for each processing bin.

LiDAR data resolution for the Musselshell AOI:

- Average Point (First Return) Density = 6.93 points/m²
- Average Ground Point Density = 0.74 points/m²

Figure 32. Density distribution for first return laser points

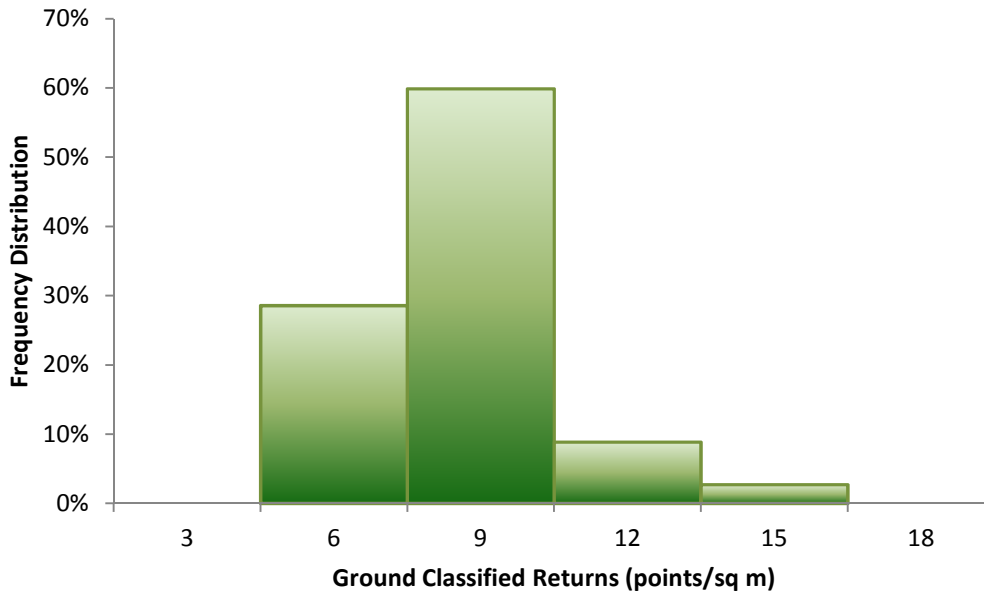


Figure 33. Density distribution for ground classified laser points

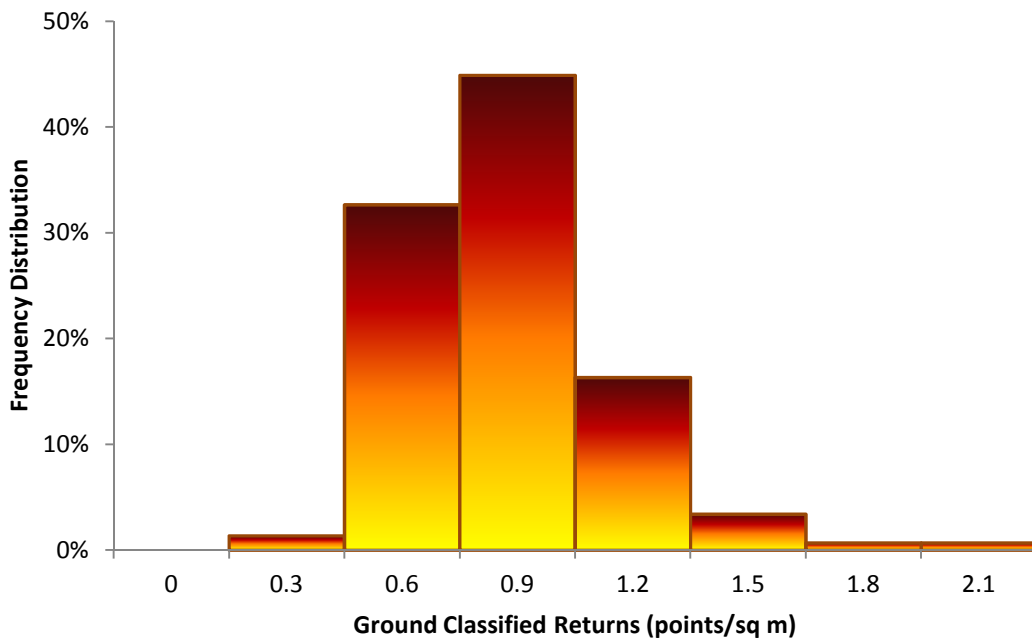
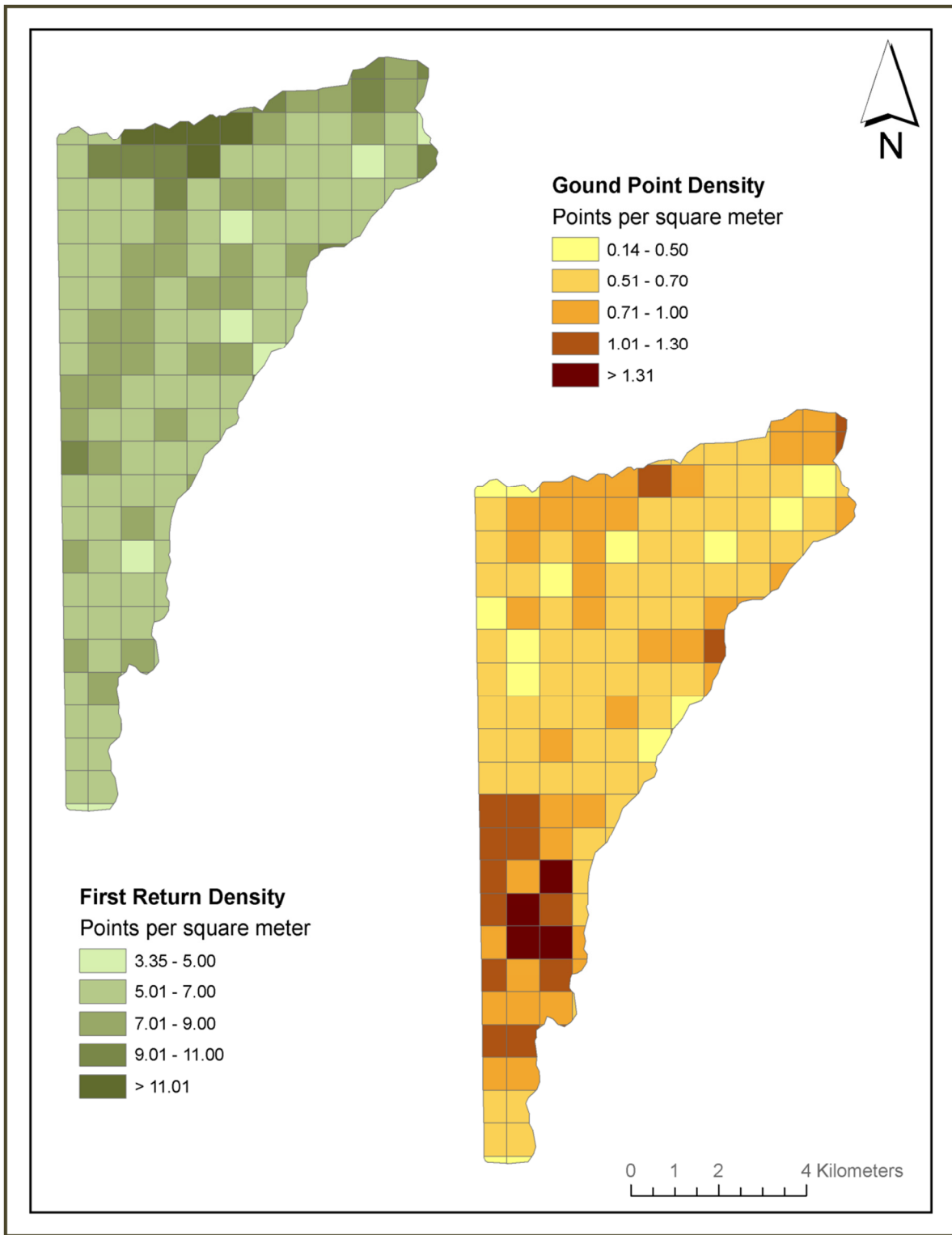


Figure 34. Density distribution map for first return points by processing bin for the Musselshell AOI

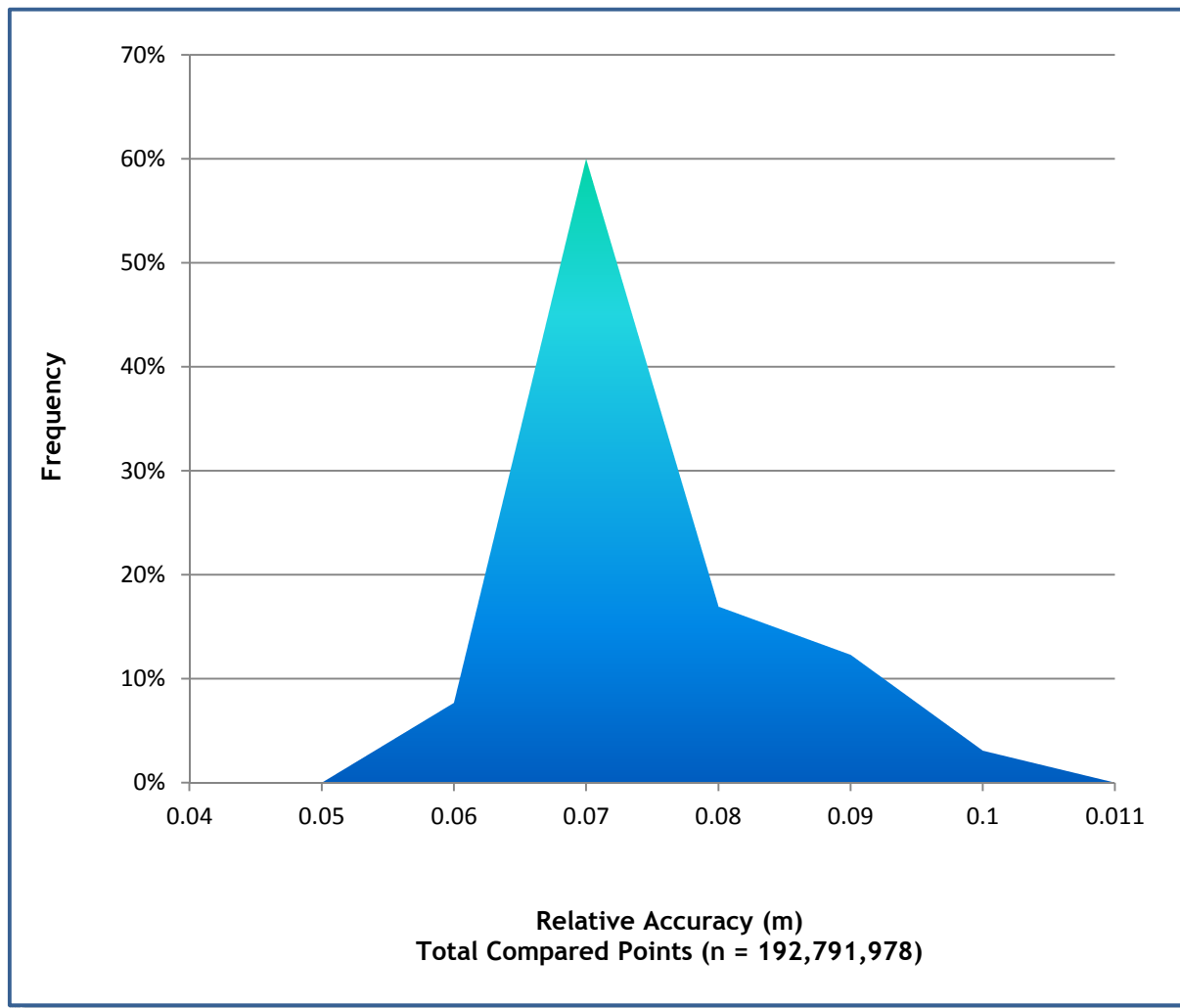


5.5.2 Relative Accuracy Calibration Results

Relative accuracy statistics for the Musselshell AOI measure the full survey calibration including areas outside the delivered boundary:

- Project Average = 0.065 m
- Median Relative Accuracy = 0.067 m
- 1σ Relative Accuracy = 0.009 m
- 1.96σ Relative Accuracy = 0.018 m

Figure 35. Distribution of relative accuracies per flight line, non slope-adjusted



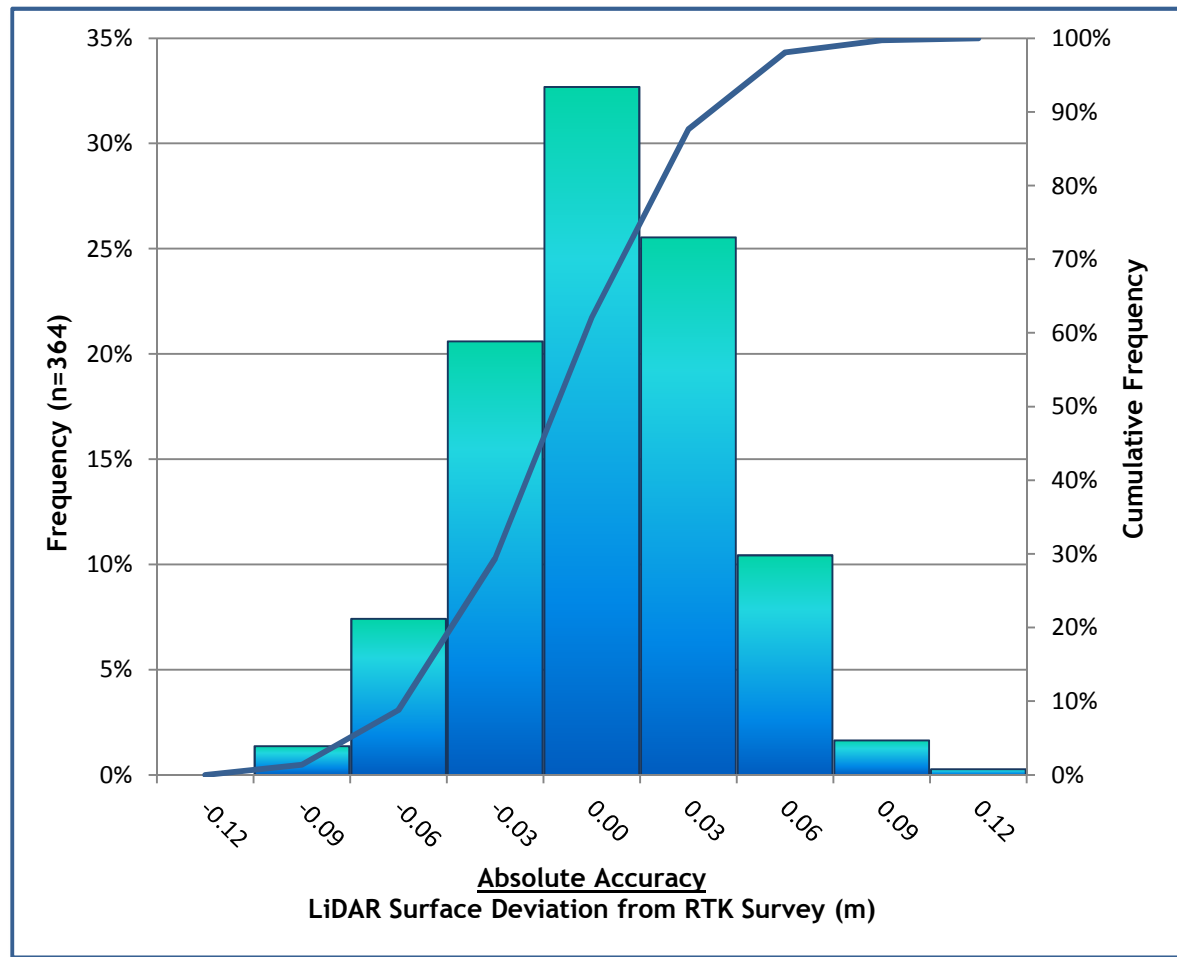
5.5.3 Absolute Accuracy

Absolute accuracies for the Musselshell AOI:

Table 15. Absolute Accuracy - Deviation between laser points and RTK hard surface survey points

RTK Survey Sample Size (n): 364	
Root Mean Square Error (RMSE) = 0.037 m	Minimum Δz = -0.116 m
Standard Deviations 1 sigma (σ): 0.036 m 1.96 sigma (σ): 0.070 m	Maximum Δz = 0.092 m
	Average Δz = -0.011 m

Figure 36. Absolute Accuracy - Histogram Statistics



5.5.4 Accuracy per Land Cover

Table 16. Summary of absolute accuracy statistics for each land cover type in the Musselshell AOI

Land cover	Sample size (n)	Mean Dz :	1 sigma (σ):	1.96 sigma (σ):	RMSE:
Gravel/Road	364	-0.011 m	0.036 m	0.070 m	0.037 m
Grass	137	0.201 m	0.164 m	0.322 m	0.265 m
Shrubs	24	0.191 m	0.130 m	0.255 m	0.230 m
Trees	29	0.063 m	0.123 m	0.241 m	0.136 m
Wetland	5	0.282 m	0.080 m	0.157 m	0.291 m

5.6 Data Summary: Priest

Table 17. LiDAR Resolution and Accuracy - Specifications and Achieved Values

	Targeted	Achieved
Resolution:	≥ 4 points/m ²	10.40 points/m ²
*Vertical Accuracy (1 σ):	<15 cm	4.9 cm

5.6.1 Data Density/Resolution

Figure 39 displays the distribution of average native and ground point densities for each processing bin.

LiDAR data resolution for the Priest AOI:

- Average Point (First Return) Density = 10.40 points/m²
- Average Ground Point Density = 0.95 points/m²

Figure 37. Density distribution for first return laser points

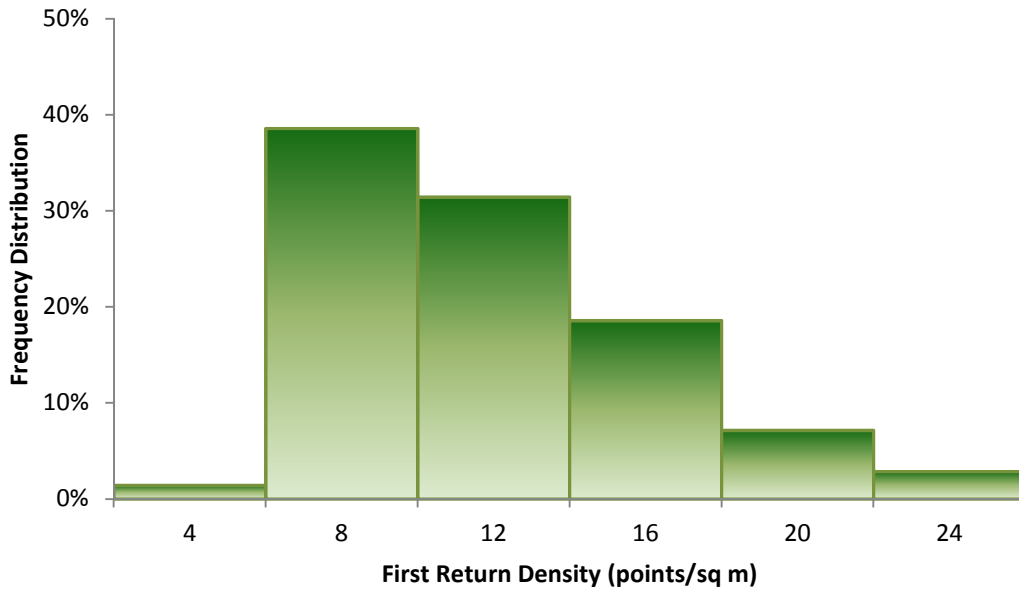


Figure 38. Density distribution for ground classified laser points

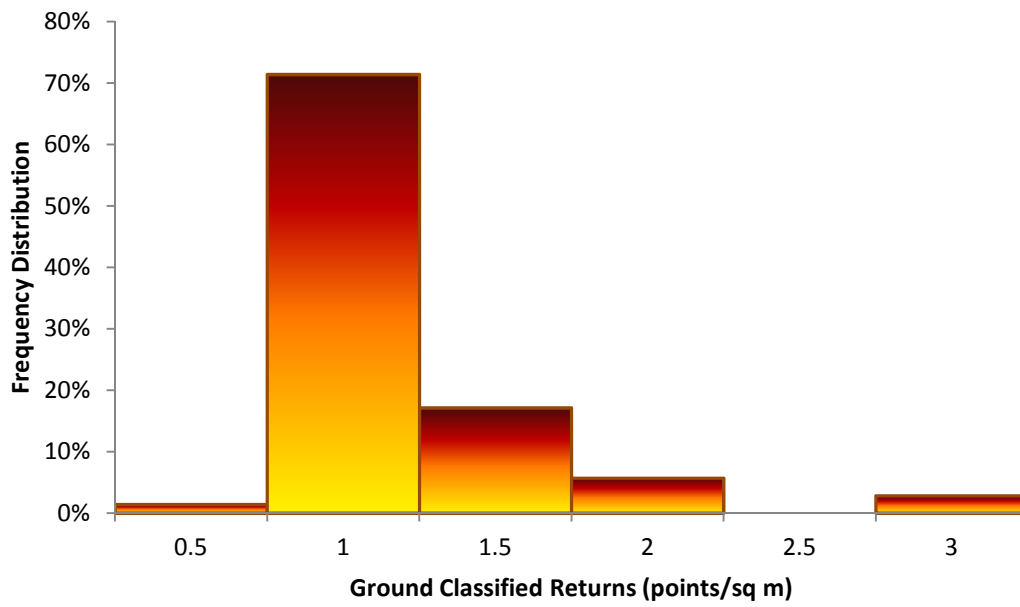
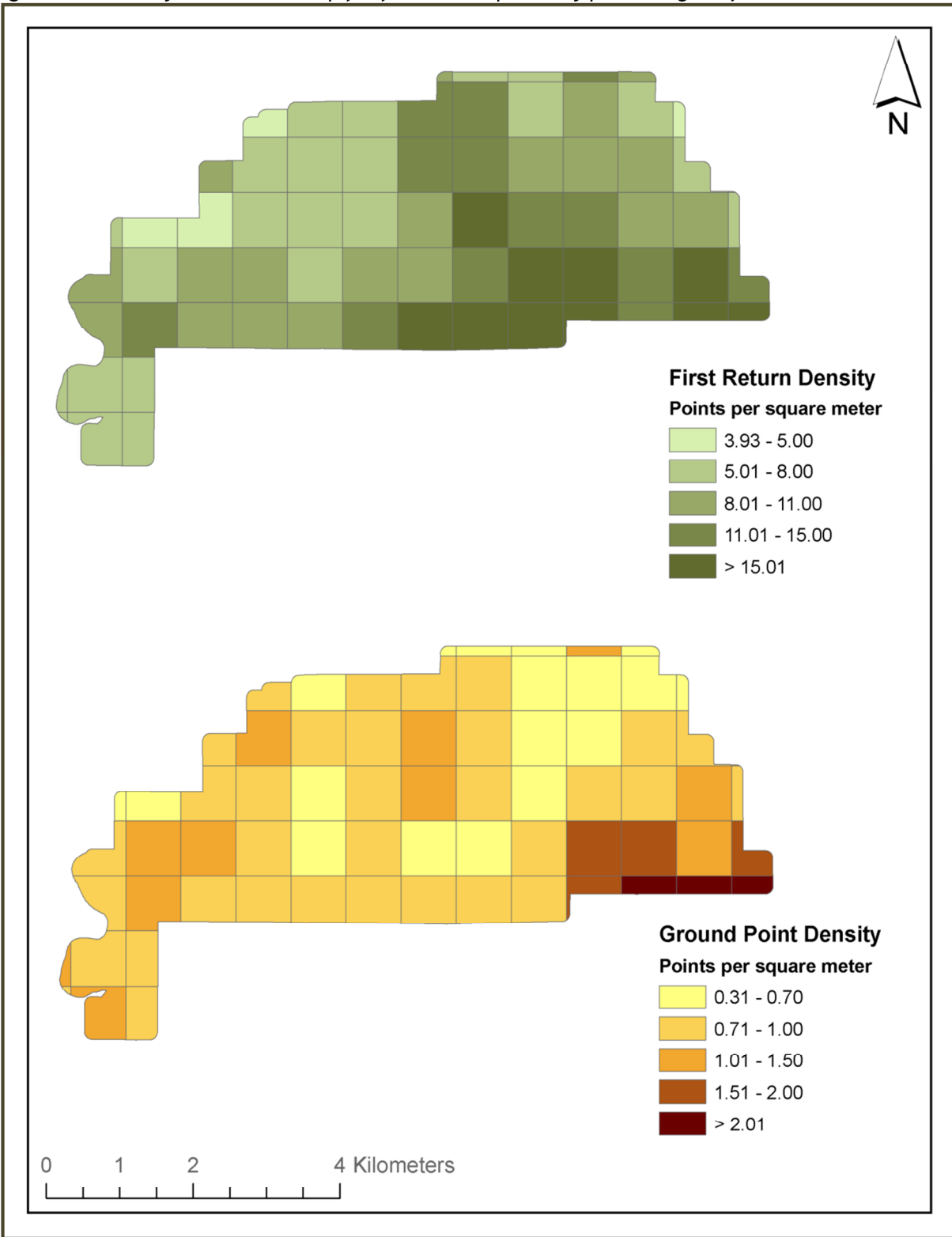


Figure 39. Density distribution map for first return points by processing bin for the Priest AOI

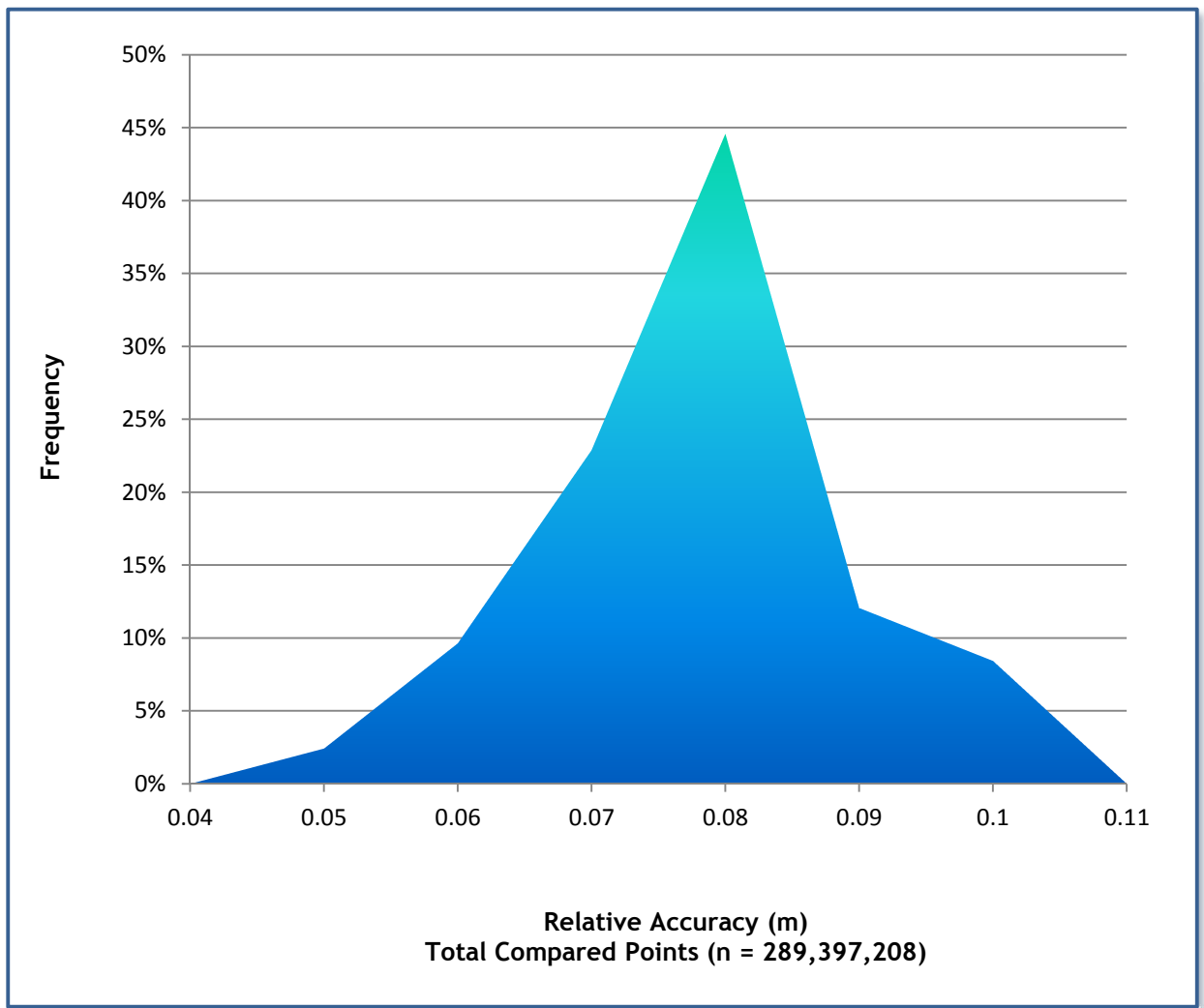


5.6.2 Relative Accuracy Calibration Results

Relative accuracy statistics for the Priest AOI measure the full survey calibration including areas outside the delivered boundary:

- Project Average = 0.073 m
- Median Relative Accuracy = 0.073 m
- 1σ Relative Accuracy = 0.011 m
- 1.96σ Relative Accuracy = 0.021 m

Figure 40. Distribution of relative accuracies per flight line, non slope-adjusted



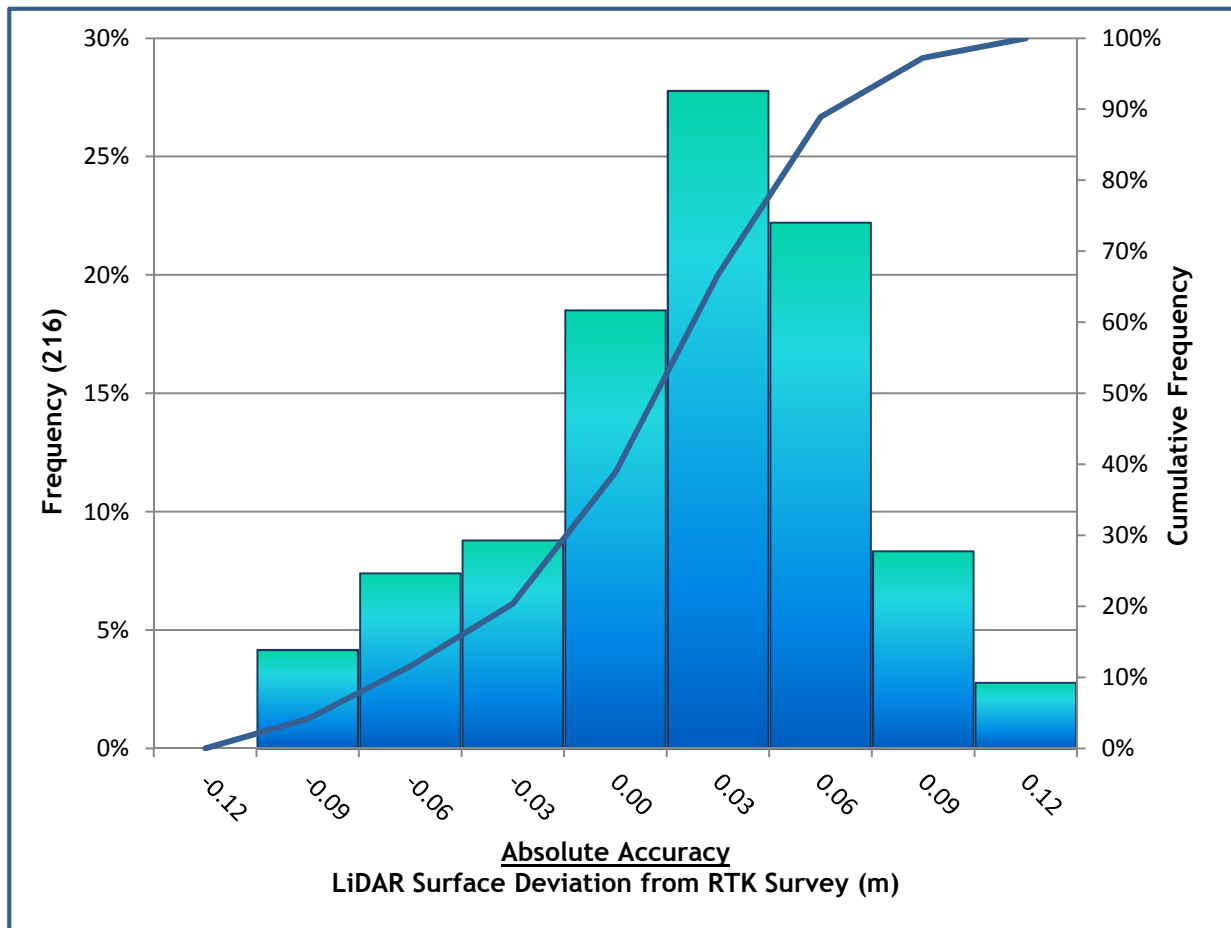
5.6.3 Absolute Accuracy

Absolute accuracies for the Priest AOI:

Table 18. Absolute Accuracy - Deviation between laser points and RTK hard surface survey points

RTK Survey Sample Size (n): 216		
Root Mean Square Error (RMSE) = 0.050 m		Minimum Δz = -0.119 m
Standard Deviations		Maximum Δz = 0.115 m
1 sigma (σ): 0.049 m	1.96 sigma (σ): 0.097 m	Average Δz = 0.008 m

Figure 41. Absolute Accuracy - Histogram Statistics



5.6.4 Accuracy per Land Cover

Table 19. Summary of absolute accuracy statistics for each land cover type in the Priest AOI

Land cover	Sample size (n)	Mean Dz :	1 sigma (σ):	1.96 sigma (σ):	RMSE:
Gravel/Road	216	0.008 m	0.049 m	0.097 m	0.050 m
Grass	28	0.249 m	0.205 m	0.402 m	0.320 m
Shrubs	26	0.570 m	0.323 m	0.633 m	0.652 m
Trees	35	0.101 m	0.100 m	0.195 m	0.141 m

5.7 Data Summary: Deception

Table 20. LiDAR Resolution and Accuracy - Specifications and Achieved Values

	Targeted	Achieved
Resolution:	≥ 4 points/m ²	8.87 points/m ²
*Vertical Accuracy (1 σ):	<15 cm	4.4 cm

5.7.1 Data Density/Resolution

Figure 44 displays the distribution of average native and ground point densities for each processing bin.

LiDAR data resolution for the Deception AOI:

- Average Point (First Return) Density = 8.87 points/m²
- Average Ground Point Density = 0.86 points/m²

Figure 42. Density distribution for first return laser points

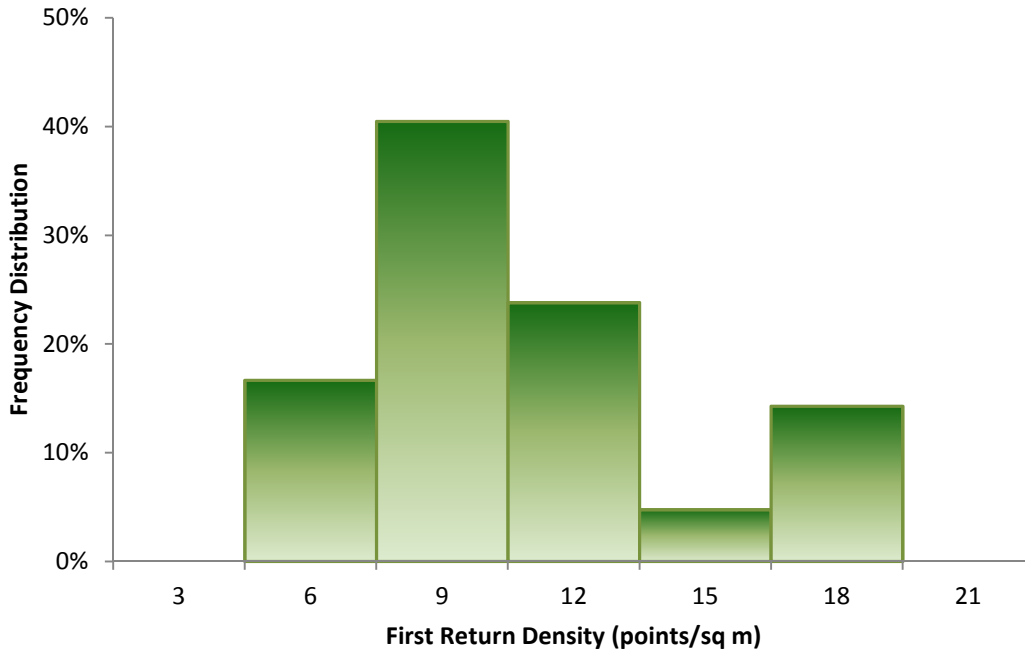


Figure 43. Density distribution for ground classified laser points

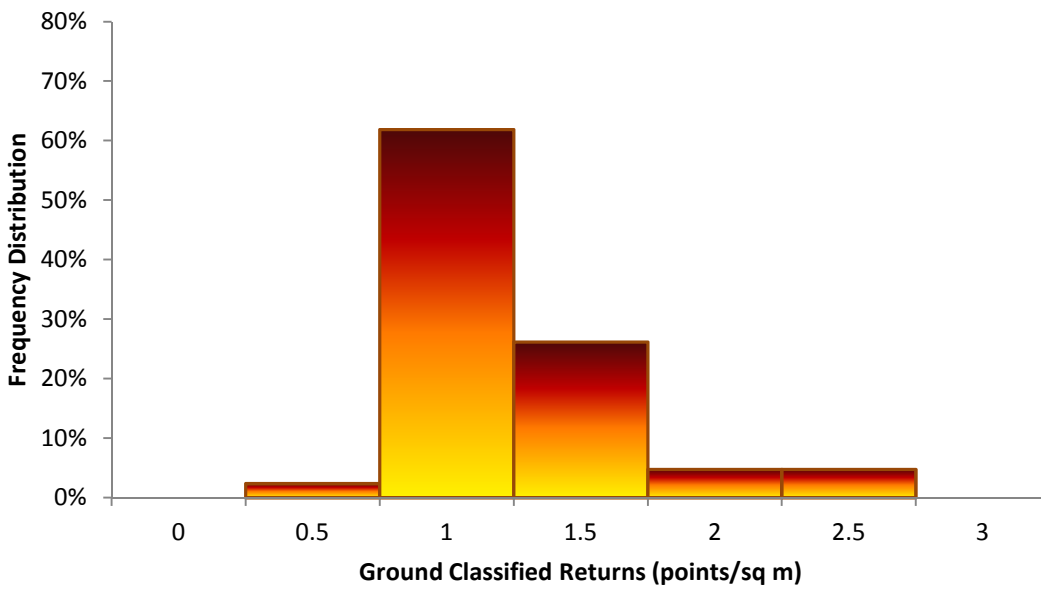
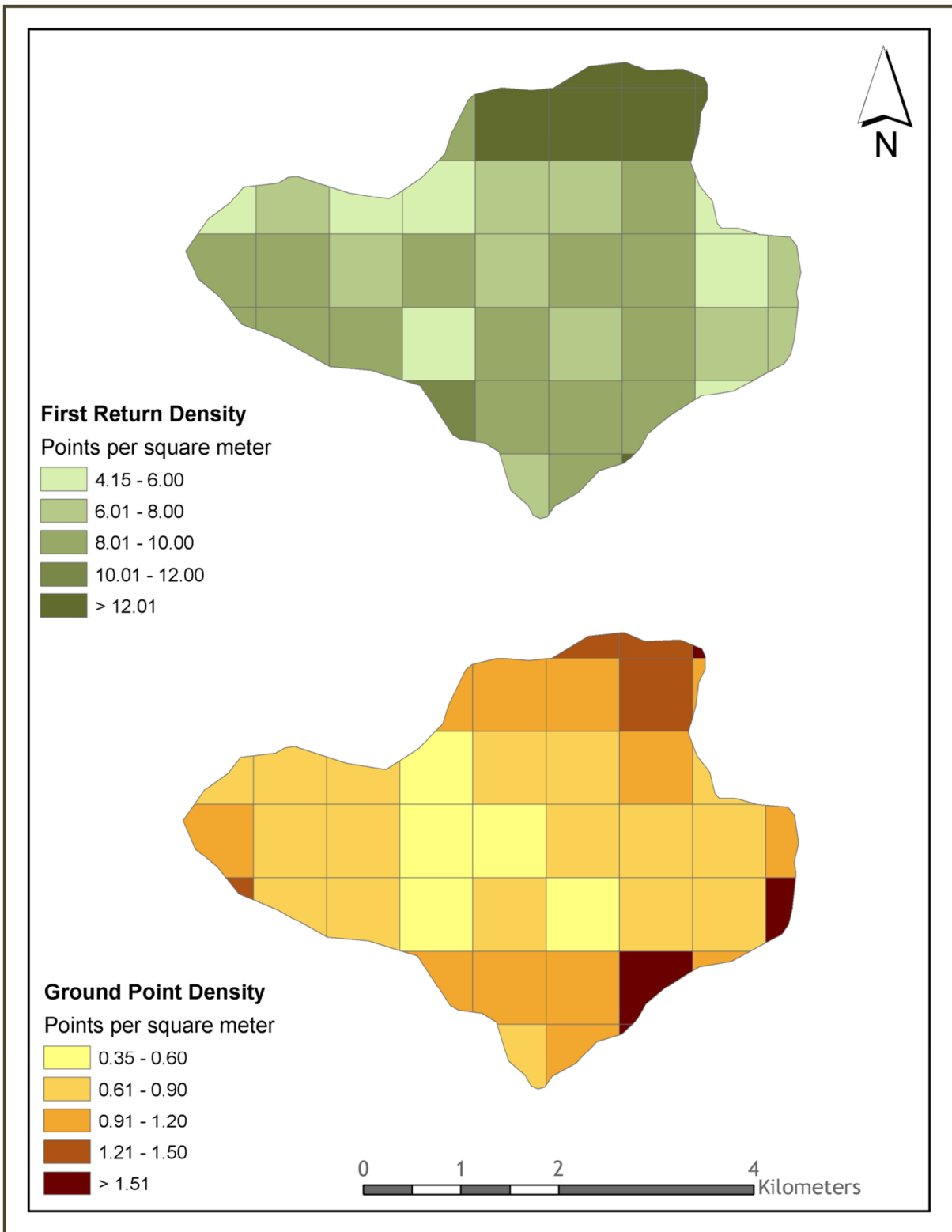


Figure 44. Density distribution map for first return points by processing bin for the Deception AOI

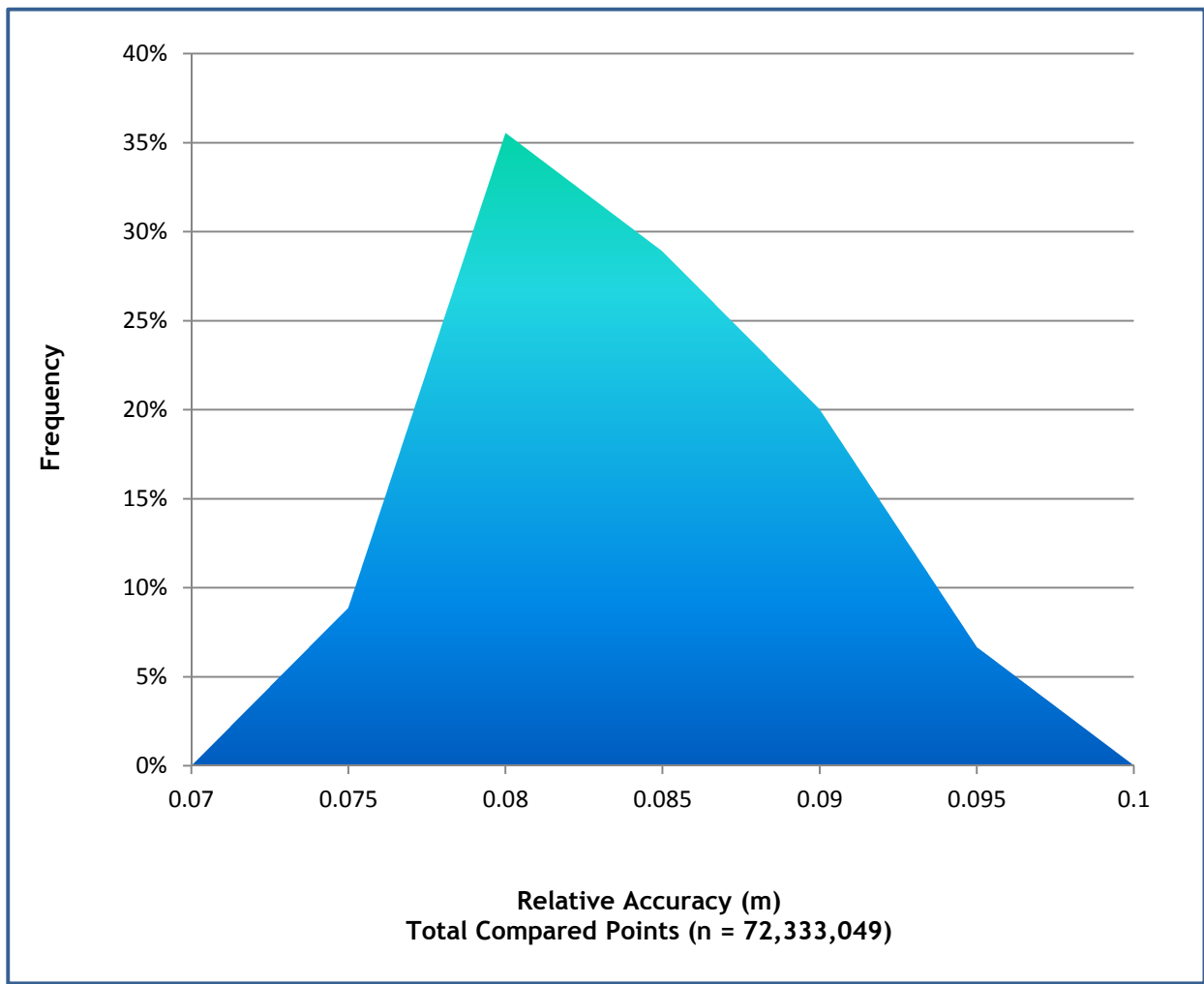


5.7.2 Relative Accuracy Calibration Results

Relative accuracy statistics for the Deception AOI measure the full survey calibration including areas outside the delivered boundary:

- Project Average = 0.081 m
- Median Relative Accuracy = 0.080 m
- 1σ Relative Accuracy = 0.005 m
- 1.96σ Relative Accuracy = 0.010 m

Figure 45. Distribution of relative accuracies per flight line, non slope-adjusted



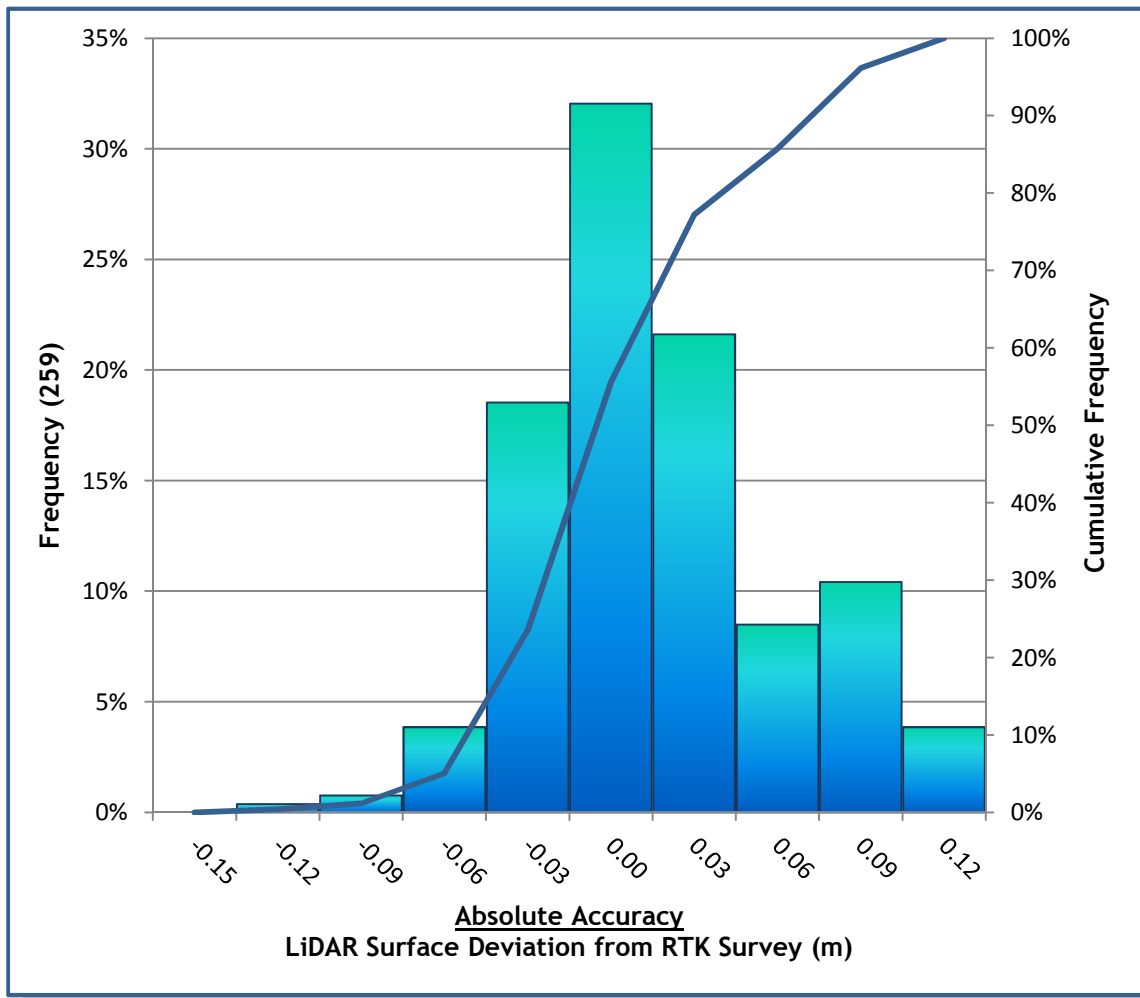
5.7.3 Absolute Accuracy

Absolute accuracies for the Deception AOI:

Table 21. Absolute Accuracy - Deviation between laser points and RTK hard surface survey points

RTK Survey Sample Size (n): 259	
Root Mean Square Error (RMSE) = 0.044 m	Minimum Δz = -0.127 m
Standard Deviations 1 sigma (σ): 0.044 m 1.96 sigma (σ): 0.086 m	Maximum Δz = 0.107 m
	Average Δz = 0.003 m

Figure 46. Absolute Accuracy - Histogram Statistics



5.7.4 Accuracy per Land Cover

Table 22. Summary of absolute accuracy statistics for each land cover type in the Deception AOI

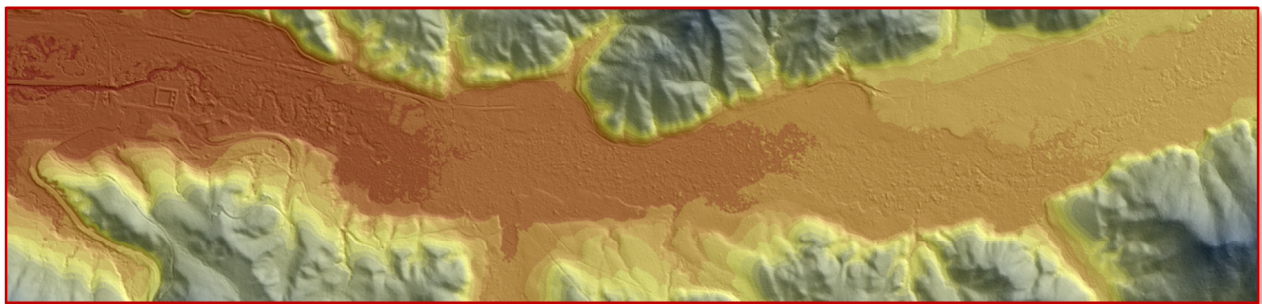
Land cover	Sample size (n)	Mean Dz :	1 sigma (σ):	1.96 sigma (σ):	RMSE:
Gravel/Road	259	0.003 m	0.044 m	0.086 m	0.044 m
Grass	28	0.095 m	0.093 m	0.183 m	0.132 m
Trees	58	0.159 m	0.255 m	0.499 m	0.298 m

6. Projection/Datum and Units

	Projection:	UTM, Zone 11
Datum	Vertical:	NAVD88 Geoid03
	Horizontal:	NAD83
	Units:	meters

7. Deliverables

Point Data:	<ul style="list-style-type: none"> • All Returns (LAS 1.2 format) • Ground Returns (LAS 1.2 format)
Vector Data:	<ul style="list-style-type: none"> • Tile Index of LiDAR Points (shapefile format) • SBETs (csv text file format)
Raster Data:	<ul style="list-style-type: none"> • Elevation Models (1m resolution) <ul style="list-style-type: none"> • Bare Earth Model (ESRI GRID and Image format) • Vegetation Model (ESRI GRID and Image format) • Intensity Images (GeoTIFF format, 0.5m resolution)
Data Report:	<ul style="list-style-type: none"> • Full report containing introduction, methodology, and accuracy • Survey Control Verification Report from Whiteshield, Inc.



8. Selected Images

Figure 47. View looking north at the northern boundary of the WPK AOI. Forest Roads 454 and 460 can be seen on the eastern slope. Top image is bare earth DEM colored by elevation, bottom image is 3D LiDAR point cloud colored by 2009 NAIP imagery.

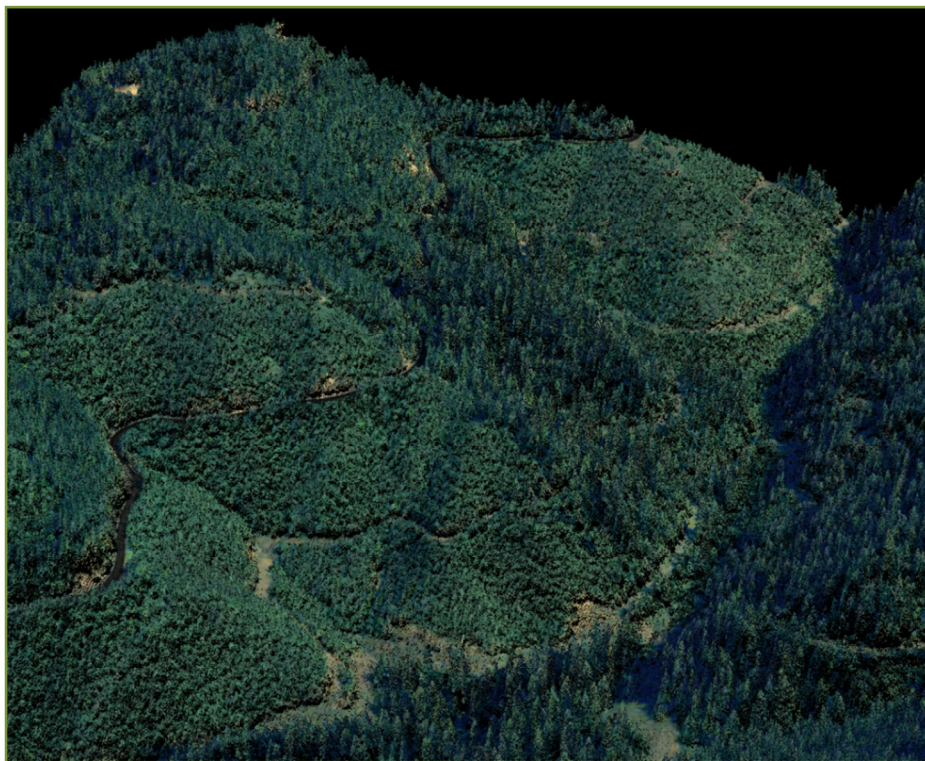
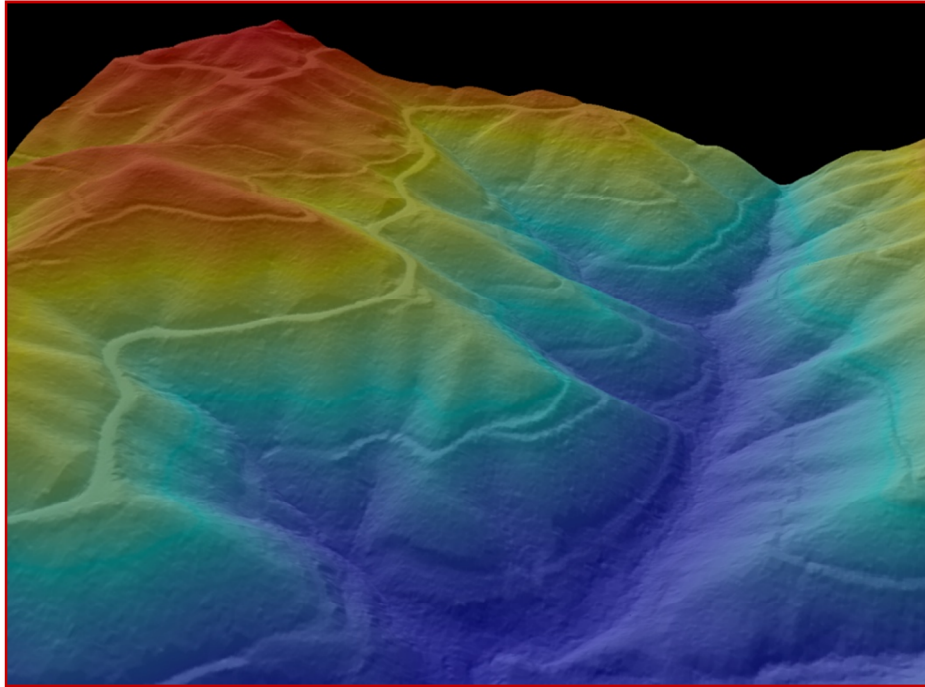


Figure 48. Intersection of Pete King Road and Hwy 12, looking northwest. Top image is bare earth DEM colored by elevation, bottom image is 3D LiDAR point cloud colored by 2009 NAIP imagery.

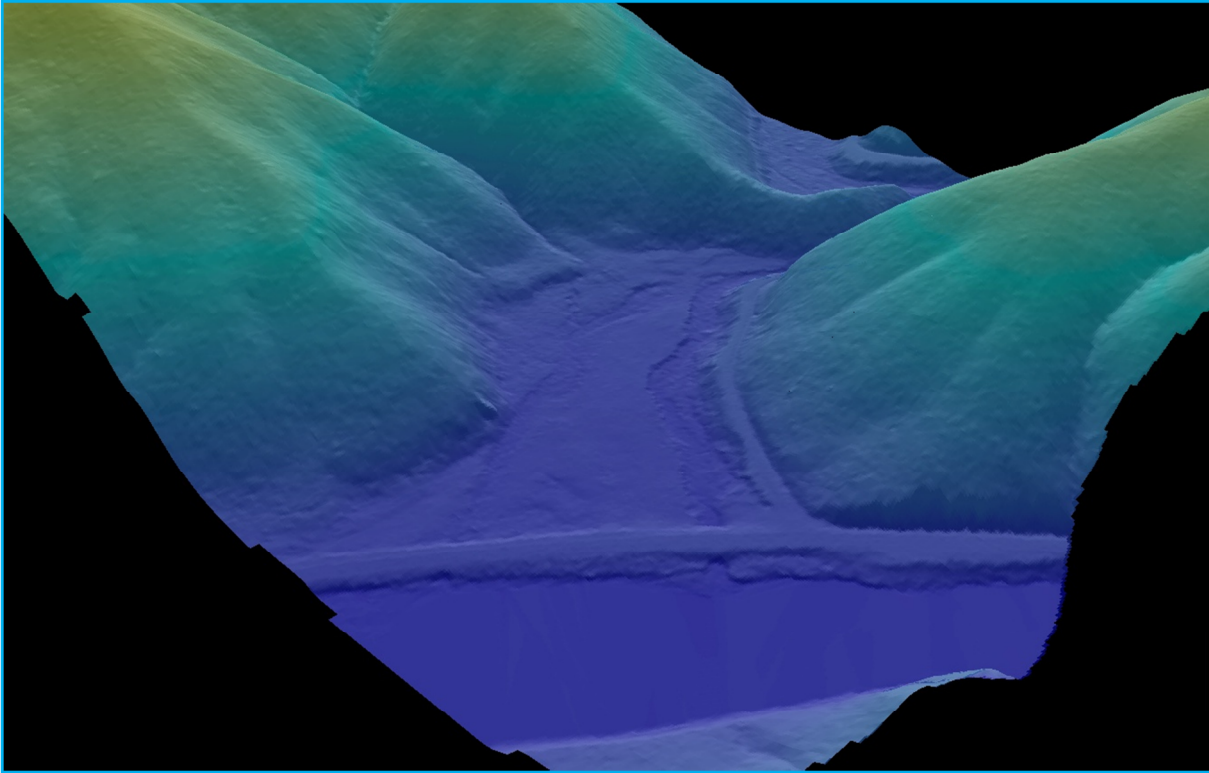


Figure 49. Clearing at the intersection of Moose Creek Rd and County Rd 754 in the China AOI. Top image is bare earth DEM colored by elevation, bottom image is 3D LiDAR point cloud colored by 2009 NAIP imagery.

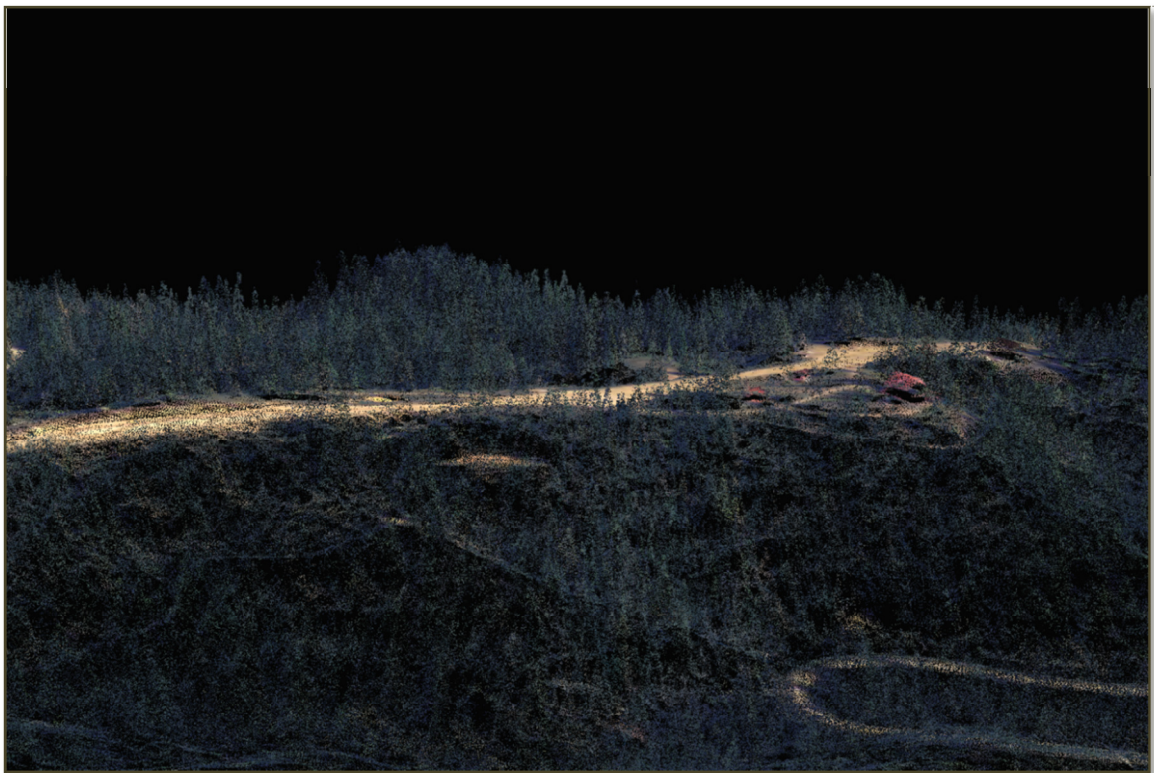
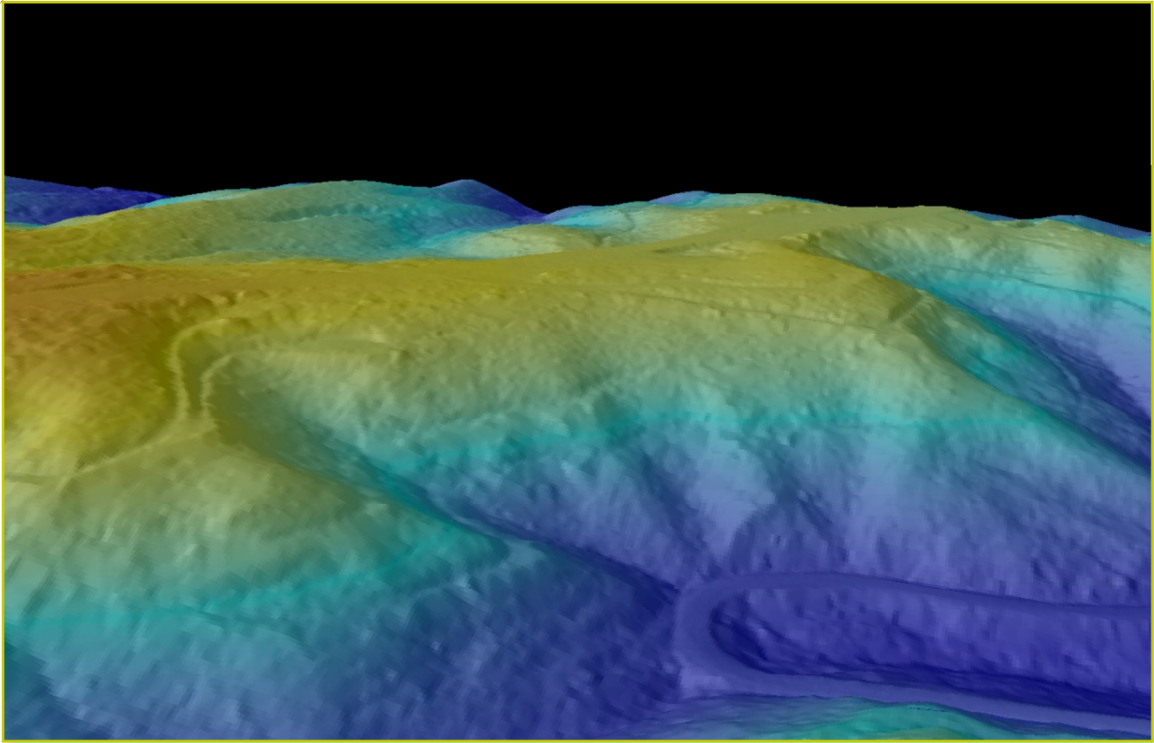


Figure 50. Northwest view of FR 74544 in the China AOI. Top image is bare earth DEM colored by elevation, bottom image is 3D LiDAR point cloud colored by 2009 NAIP imagery.

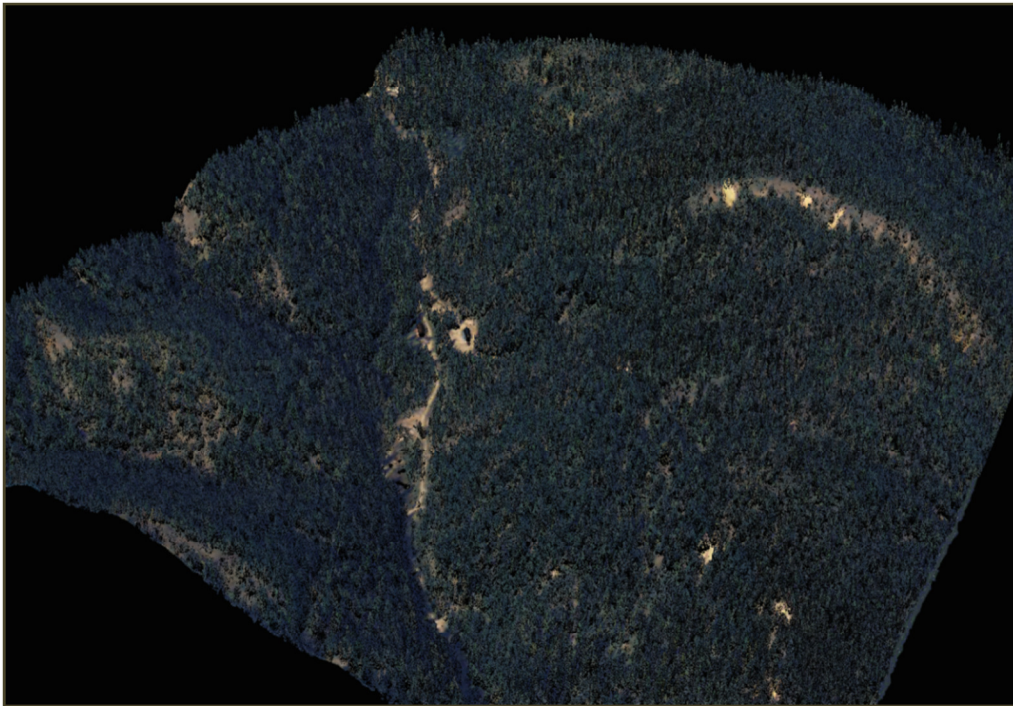
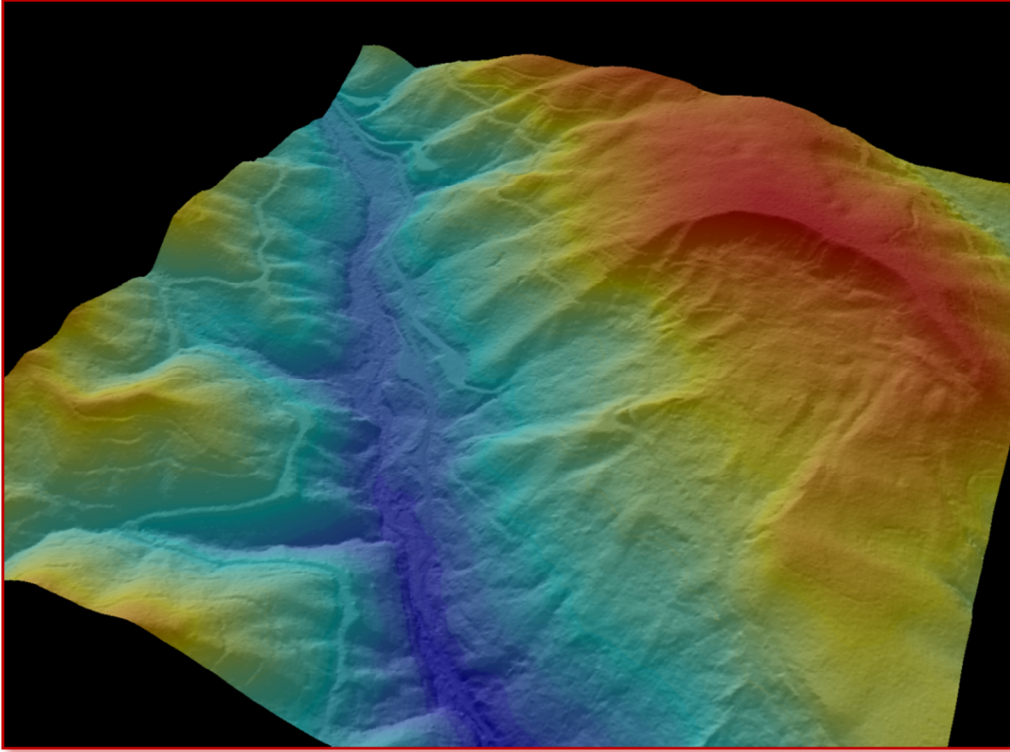


Figure 51. Top image is a west looking view of the confluence of the west fork Potlatch River with the mainstem Potlatch River, image is a 3D LiDAR point cloud colored by 2009 NAIP imagery. Bottom image is a close of the same riparian area, and is a 3D LiDAR point cloud colored by elevation



9. Glossary

1-sigma (σ) Absolute Deviation: Value for which the data are within one standard deviation (approximately 68th percentile) of a normally distributed data set.

1.96-sigma (σ) Absolute Deviation: Value for which the data are within two standard deviations (approximately 95th percentile) of a normally distributed data set.

Root Mean Square Error (RMSE): A statistic used to approximate the difference between real-world points and the LiDAR points. It is calculated by squaring all the values, then taking the average of the squares and taking the square root of the average.

Pulse Rate (PR): The rate at which laser pulses are emitted from the sensor; typically measured as thousands of pulses per second (kHz).

Pulse Returns: For every laser pulse emitted, the Leica ALS 50 Phase II system can record *up to four* wave forms reflected back to the sensor. Portions of the wave form that return earliest are the highest element in multi-tiered surfaces such as vegetation. Portions of the wave form that return last are the lowest element in multi-tiered surfaces.

Accuracy: The statistical comparison between known (surveyed) points and laser points. Typically measured as the standard deviation (sigma, σ) and root mean square error (RMSE).

Intensity Values: The peak power ratio of the laser return to the emitted laser. It is a function of surface reflectivity.

Data Density: A common measure of LiDAR resolution, measured as points per square meter.

Spot Spacing: Also a measure of LiDAR resolution, measured as the average distance between laser points.

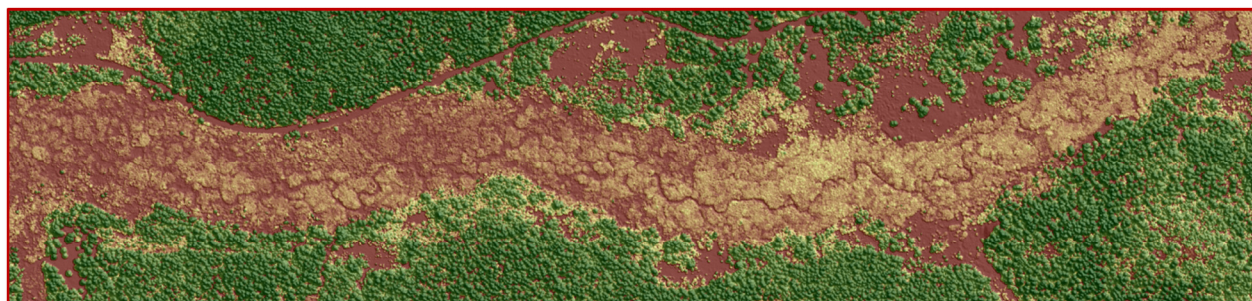
Nadir: A single point or locus of points on the surface of the earth directly below a sensor as it progresses along its flight line.

Scan Angle: The angle from nadir to the edge of the scan, measured in degrees. Laser point accuracy typically decreases as scan angles increase.

Overlap: The area shared between flight lines, typically measured in percents; 100% overlap is essential to ensure complete coverage and reduce laser shadows.

DTM / DEM: These often-interchanged terms refer to models made from laser points. The digital elevation model (DEM) refers to all surfaces, including bare ground and vegetation, while the digital terrain model (DTM) refers only to those points classified as ground.

Real-Time Kinematic (RTK) Survey: GPS surveying is conducted with a GPS base station deployed over a known monument with a radio connection to a GPS rover. Both the base station and rover receive differential GPS data and the baseline correction is solved between the two. This type of ground survey is accurate to 1.5 cm or less.



10. Citations

Soininen, A. 2004. TerraScan User's Guide. TerraSolid.

Appendix A

LiDAR accuracy error sources and solutions:

Type of Error	Source	Post Processing Solution
GPS (Static/Kinematic)	Long Base Lines	None
	Poor Satellite Constellation	None
	Poor Antenna Visibility	Reduce Visibility Mask
Relative Accuracy	Poor System Calibration	Recalibrate IMU and sensor offsets/settings
	Inaccurate System	None
Laser Noise	Poor Laser Timing	None
	Poor Laser Reception	None
	Poor Laser Power	None
	Irregular Laser Shape	None

Operational measures taken to improve relative accuracy:

1. Low Flight Altitude: Terrain following is employed to maintain a constant above ground level (AGL). Laser horizontal errors are a function of flight altitude above ground (i.e., ~ 1/3000th AGL flight altitude).
2. Focus Laser Power at narrow beam footprint: A laser return must be received by the system above a power threshold to accurately record a measurement. The strength of the laser return is a function of laser emission power, laser footprint, flight altitude and the reflectivity of the target. While surface reflectivity cannot be controlled, laser power can be increased and low flight altitudes can be maintained.
3. Reduced Scan Angle: Edge-of-scan data can become inaccurate. The scan angle was reduced to a maximum of $\pm 15^\circ$ from nadir, creating a narrow swath width and greatly reducing laser shadows from trees and buildings.
4. Quality GPS: Flights took place during optimal GPS conditions (e.g., 6 or more satellites and PDOP [Position Dilution of Precision] less than 3.0). Before each flight, the PDOP was determined for the survey day. During all flight times, a dual frequency DGPS base station recording at 1-second epochs was utilized and a maximum baseline length between the aircraft and the control points was less than 19 km (11.5 miles) at all times.
5. Ground Survey: Ground survey point accuracy (i.e. <1.5 cm RMSE) occurs during optimal PDOP ranges and targets a minimal baseline distance of 4 miles between GPS rover and base. Robust statistics are, in part, a function of sample size (n) and distribution. Ground survey RTK points are distributed to the extent possible throughout multiple flight lines and across the survey area.
6. 50% Side-Lap (100% Overlap): Overlapping areas are optimized for relative accuracy testing. Laser shadowing is minimized to help increase target acquisition from multiple scan angles. Ideally, with a 50% side-lap, the most nadir portion of one flight line coincides with the edge (least nadir) portion of overlapping flight lines. A minimum of 50% side-lap with terrain-followed acquisition prevents data gaps.
7. Opposing Flight Lines: All overlapping flight lines are opposing. Pitch, roll and heading errors are amplified by a factor of two relative to the adjacent flight line(s), making misalignments easier to detect and resolve.